Loop Approach to Lattice Gauge Theories

Manu Mathur[1]

S. N. Bose National Centre for Basic Sciences

JD Block, Sector III, Salt Lake City, Calcutta 98, India.

arXiv:hep-lat/0702007v3 7 May 2007

Abstract

We solve the Gauss law and the corresponding Mandelstam constraints in the loop Hilbert space $\mathcal{H}^L$ using the prepotential formulation of $(d+1)$ dimensional SU(2) lattice gauge theory. The resulting orthonormal and complete loop basis, explicitly constructed in terms of the $d(2d-1)$ prepotential intertwining operators, is used to transcribe the gauge dynamics directly in $\mathcal{H}^L$ without any redundant gauge and loop degrees of freedom. Using generalized Wigner-Eckart theorem and Biedenharn -Elliot identity in $\mathcal{H}^L$, we show that the above loop dynamics for pure SU(2) lattice gauge theory in arbitrary dimension, is given by real and symmetric $3nj$ coefficients of the second kind (e.g., n=6, 10 for d=2, 3 respectively). The corresponding "ribbon diagrams" representing SU(2) loop dynamics are constructed. The prepotential techniques are trivially extended to include fundamental matter fields leading to a description in terms of loops and strings. The SU(N) gauge group is briefly discussed.

1 Introduction

The idea that gauge theories should be formulated completely in terms of loops in space carrying electric fluxes is quite old, appealing and has long history [1, 2, 3, 4, 5, 6]. In the context of electrodynamics, Yang [3] has emphasized the importance of path dependent "non-integrable phase factors" carrying electric fluxes to provide a complete description of all the quantum effects. In the context of quantum chromodynamics the loop formulation, without any colored gluon or colored quark degrees of freedom, is further expected to provide a better framework to analyze non-perturbative low energy issues like color confinement. In the context of gravity, the relatively recent Hamiltonian formulation of quantum gravity in terms of SU(2) connections has also been reformulated in terms of loops leading to loop quantum gravity [7]. Therefore, the loop formulation of gauge theories may eventually provide a common geometrical platform to understand all interactions in nature. In this work, we analyze some of the basic kinematical as well as dynamical issues involved in the Hamiltonian formulation of lattice gauge theories in terms of loops.

The standard construction of the loop states for pure SU(N) gauge theory on lattice [5] consists of considering the set of all oriented loops Γ and constructing the corresponding gauge invariant Wilson loop operators $W_\gamma \equiv \mathrm{Tr}U_\gamma$ for every $\gamma \in \Gamma$. Acting on the strong coupling vacuum, all possible gauge invariant operators of the form $W_{\gamma_1}W_{\gamma_2}....W_{\gamma_m}$ create all possible gauge invariant states associated with the corresponding loops $\gamma_1\gamma_2...\gamma_m$. These loop states are manifestly gauge invariant, geometrical and form a basis, usually known as Wilson loop basis (see section 2.1). However, a serious problem with

[1]E. Mail: manu@bose.res.in

this Wilson loop basis is that it again over-describes gauge theory. This time, the over description is because loops of all shapes and sizes have to be included in constructing the above loop basis. Therefore, one is again confronted with too many redundant (but now SU(N) gauge invariant) loop degrees of freedom (see section 2.1). The Mandelstam constraints [1] amongst the various loop states express this over-completeness of the Wilson loop basis (see section 2.1). As these constraints represent the linear dependence of the gauge invariant states associated with loops of all sizes, they are highly non-local and hence difficult to solve (see section 2.1). In the strong coupling ($g \to \infty$) limit, the loops are small and they carry small electric fluxes [5]. Therefore, the Mandelstam constraints can be easily solved by using Gram-Schmidt orthogonalization procedure amongst the small number of loop states considered within this ($g \to \infty$) limit. However, in the continuum ($g \to 0$) limit, as opposed to the strong coupling limit, large loops carrying large electric fluxes will be important [15]. Therefore, the problem of over-completeness of the Wilson loop basis will become more and more acute as we remove the lattice cut-off and approach the continuum limit. This over-completeness, in turn, will result in rapid proliferation of spurious zero modes of the Hamiltonian in the Wilson loop basis. Therefore, the initial problem in loop formulation is to solve the Mandelstam constraints *exactly* before addressing any dynamical issue. Infact, as stated by Gambini and Pullin in [8][2]: "*The proliferation of loops when one considers larger lattices and higher dimensions completely washes out the advantages provided by the (loop) formalism.*".

The motivation and purpose of the present work is to systematically develop ideas and techniques to reformulate lattice gauge theories in loop space without any spurious loop degrees of freedom. We solve SU(2) Mandelstam constraints leading to an orthonormal loop basis which is complete and characterized exactly by $3(d-1)$ angular momentum quantum numbers per lattice site [10]. Further, we show that the most economical description of the pure $(d+1)$ SU(2) lattice gauge theory dynamics, involving only the relevant loop degrees of freedom, is given by $3nj$ coefficients of the second kind and therefore it is highly geometrical.

We will work within the prepotential formulation [9, 10] of SU(2) lattice gauge theory Hamiltonian [5]. The prepotential approach has extended $SU(2) \otimes U(1)$ gauge invariance. The prepotential operators are SU(2) harmonic oscillator doublets attached to the initial and the final points of every link. They are connected by the U(1) gauge invariance mentioned above (see section 2.2). The advantage of prepotential approach is that the non-local and over-complete Wilson loop basis can be constructed and studied locally in terms of the SU(2) invariant $d(2d-1)$ "prepotential intertwining operators" at every lattice site. This local description of the Wilson loop basis is characterized by $2d(d-1)$ (integer) intertwining quantum number per lattice site. Further, the Mandelstam constraints, which appear highly non-local in terms of the link operators, become local in terms of the prepotential operators (see section 2.3.1). This enables us to solve them explicitly using simple group theoretical ideas [11, 12]. The novel U(1) gauge invariance of the prepotential formulation then enables us to explicitly construct an *orthonormal and complete loop basis* in the entire loop Hilbert space $\mathcal{H}^L$ on the lattice. As expected, this orthonormal basis is characterized by $3(d-1)$ (as opposed to $2d(d-1)$ quantum numbers for the Wilson loop basis) gauge invariant quantum numbers per lattice site. Having solved all the constraints, we use the generalized Wigner-Eckart theorem and Biedenharn-Elliot identities in

[2] Chapter 12, page 303-304

the resulting orthonormal loop basis to compute the loop dynamics. Our approach also enables us to compute loop dynamics locally site by site. The final results at different lattice site are then glued together through the U(1) gauge invariance. We show that in $d+1$ dimension the SU(2) loop dynamics in the (I, J) plane where $I, J = 1.....d$ and $I < J$ plane is given by $3nj$ coefficients of the second kind where $n = 2\,[2 + d + (J - I) - \delta_{I,1} - \delta_{J,d}]$. The matrix elements of the Hamiltonian in the above loop basis are found to be real and symmetric. The $3nj$ coefficients of second kind, and therefore the loop dynamics, are graphically represented by the ribbon diagrams.

The plan of the paper is as follows. In the first half (section 2) we discuss the kinematical issues and in the second half (section 3) we discuss the dynamical issues. In both these sections, the explicit computations are done in $d = 2$. This keeps the discussions simple and also illustrates all the essential ideas and techniques involving prepotentials. Their generalization to arbitrary d dimension is obvious and done next. As the complications caused by over-completeness of the loop basis or equivalently the Mandelstam constraints have been major obstacles in the loop approach to gauge theories, we first review them on lattice in section 2.1. In section 2.2, we briefly discuss the $SU(2) \otimes U(1)$ gauge invariant prepotential approach [9] which enables us to cast the Mandelstam constraints in a simple local form. In section 2.3, we solve the Mandelstam constraints and give all possible orthonormal loop state solutions [10] in terms of the $d(2d - 1)$ prepotential intertwining operators. In section 2.4, we discuss inclusion of matter fields leading to a gauge theory description in terms of loops and strings. In section 3.1 and 3.2, we compute the matrix elements of the Hamiltonian in the above loop basis and discuss the ribbon diagrams representing these amplitudes. In section 4, SU(N) gauge group is briefly discussed. The techniques used in constructing the orthonormal loop state basis are given in appendix A. The technical details involved in computing loop dynamics are given in appendix B.

2 The kinematical issues

This section is devoted to the kinematical issues involving the loop states in pure SU(2) lattice gauge theory. We first discuss the Mandelstam constraints in terms of the original lattice link operators. They look highly non-local. We then cast them in their local form at every lattice site n in terms of the SU(2) invariant prepotential intertwining operators at n. Next, we convert the problem of solving these *local* Mandelstam constraints to the problem of finding common (orthonormal) eigenvectors of a complete set of commuting observables (C.S.C.O) containing $(4d - 3)$ angular momentum operators at n. In particular, we show that the states related by the Mandelstam constraints at n are degenerate with respect to a subset of operators belonging to the above C.S.C.O.. Therefore, the common eigenvectors of the C.S.C.O at n, which are specific linear combinations of the states related by the Mandelstam constraints, lead us to an orthonormal local basis at n. The final orthonormal loop basis over the entire lattice, characterized by $3(d - 1)$ angular momentum quantum numbers per lattice site, is obtained by weaving or gluing these local orthonormal basis at different lattice sites according to the additional U(1) Gauss law associated with the prepotential formulation.

2.1 Mandelstam constraints on lattice

On lattice the number of gauge invariant degrees of freedom ($\mathcal{N}$) is given by the dimension of the quotient space $\otimes_{links} SU(2)/\otimes_{sites} SU(2)$. Thus for a d-dimensional periodic lattice with n^d sites and dn^d links:

$$\mathcal{N} = 3(d-1)n^d. \tag{1}$$

Therefore, a complete description of the SU(2) gauge invariant physical Hilbert space on a periodic lattice should require $\mathcal{N}$ quantum numbers or equivalently $3(d-1)$ quantum numbers per lattice site. However, the Wilson loop basis is characterized by $\mathcal{M} = 2d(d-1)n^d$ linking or intertwining quantum numbers (see section 2.3). Thus there are $\mathcal{M} - \mathcal{N} = \left(2d^2 - 5d + 3\right) n^d$ redundant degrees of freedom. This clearly establishes that the Wilson loop basis is over-complete. Further, the redundant degrees of freedom or degree of over-completeness increases as d^2 for large d. Let us illustrate this over-completeness by giving the simplest example in $d = 2$. We consider two plaquettes A and B touching each other at a common lattice site n as shown in Figure (1a). The corresponding Wilson loop operators satisfy:

$$\left(\mathrm{Tr}U_A\right)\left(\mathrm{Tr}U_B\right) \equiv \mathrm{Tr}\left(U_A U_B\right) + \mathrm{Tr}\left(U_A U_B^{-1}\right). \tag{2}$$

The relation (2) is a trivial identity involving any two SU(2) matrices U_A and U_B. It can be checked by writing $U_X = X_0 1 + i\sum_{a=1}^{3} X_a \sigma^a$ where σ^a are the Pauli matrices, X_0, X_a are real and satisfy $X_0^2 + X_1^2 + X_2^2 + X_3^2 = 1$. The generalisations of the identity (2) to the other classical Lie groups have been discussed in [13]. We define the following three loop states:

$$|\gamma_1\rangle \equiv \left(\mathrm{Tr}U_A\right)\left(\mathrm{Tr}U_B\right)|0\rangle, \qquad |\gamma_2\rangle \equiv \mathrm{Tr}\left(U_A U_B^{-1}\right)|0\rangle, \qquad |\gamma_3\rangle \equiv \mathrm{Tr}\left(U_A U_B\right)|0\rangle, \tag{3}$$

The identity (2) implies the simplest Mandelstam constraints:

$$|\gamma_1\rangle = |\gamma_2\rangle + |\gamma_3\rangle. \tag{4}$$

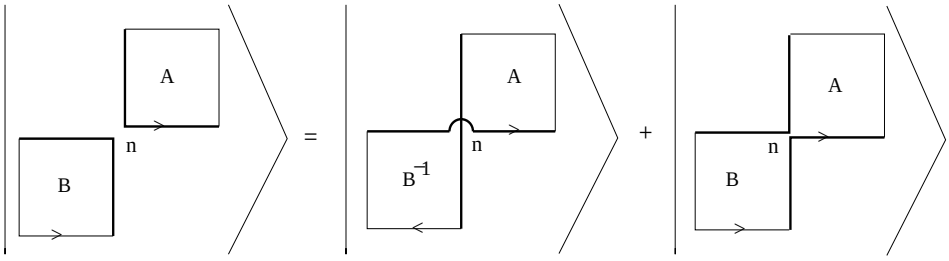

Figure 1: The graphical representation of the simplest Mandelstam constraint (4) with $N_A = N_B = 1$. The thick lines are for the later comparison of the same in the prepotential formulation.

Thus we see that the three loop states $|\gamma_1\rangle, |\gamma_2\rangle$ and $|\gamma_3\rangle$ are linearly dependent. To appreciate the problem further, let us consider most general loop states involving only these two plaquettes A and B:

$$\begin{aligned}
|N_A, N_B\rangle &\equiv (\mathrm{Tr}U_A)^{N_A}(\mathrm{Tr}U_B)^{N_B}|0\rangle \\
&= (\mathrm{Tr}U_A)^{N_A-1}(\mathrm{Tr}U_B)^{N_B-1}(\mathrm{Tr}U_AU_B + \mathrm{Tr}U_AU_B^{-1})|0\rangle \\
&= (\mathrm{Tr}U_A)^{N_A-2}(\mathrm{Tr}U_B)^{N_B-2}(\mathrm{Tr}U_AU_B + \mathrm{Tr}U_AU_B^{-1})^2|0\rangle \\
&\cdot \\
&\cdot \\
&= (\mathrm{Tr}U_A)^{N_A-N_{min}}(\mathrm{Tr}U_B)^{N_B-N_{min}}(\mathrm{Tr}U_AU_B + \mathrm{Tr}U_AU_B^{-1})^{N_{min}}|0\rangle \qquad (5)
\end{aligned}$$

where N_A, N_B are two arbitrary integers representing the angular momentum fluxes over A and B and $N_{\min}$=Minimum(N_A, N_B). Thus, given the loop state $|N_A, N_B\rangle$, we have produced $(2N_{\min}+1)$ distinct but linearly dependent Wilson loop states contained in the relations (5). Therefore, even in $d = 2$, for the simplest loop states over the two plaquettes, the number of linearly dependent loop states increases with the SU(2) flux value $N_{\min}$. Note that we have to include states with N_{min} taking arbitrarily large values. Next one can imagine extending the picture in Figure (1) by adding more plaquettes leading to further constraints[3]. In general, *one has to address the problem of finding a complete set of linearly independent loop states amongst the loop states of all shapes, sizes carrying arbitrary fluxes and touching/crossing one another at arbitrary number of lattice sites.* Further, it is clear that this problem becomes more and more difficult as the dimension d increases. This is the reason why the Mandelstam constraints have been notorious and major obstacle in the development of the loop formulation of gauge theories [8]. The solutions of the Mandelstam constraints have been discussed at various levels of approximations and difficulties in the past. In [8, 19] an approximate loop cluster method in 2+1 dimensions is developed and the Schrödinger equation is written down as difference equations in these cluster coordinates. However, approximations involved are uncontrolled [8] to enable us to go to 3+1 dimensions. Motivated by strong coupling expansions, various methods involving cluster of loops and their truncations to define Hamiltonian eigenvalue problem have been developed to go beyond strong coupling region [20]. In [21] the Mandelstam constraints are solved and eigenvalues equations are analyzed on computer using small lattices and small loops. In [22, 23] the Mandelstam constraints are solved classically on a finite periodic d=2, 3 lattice leading to an independent loop configuration space. However, the issues like quantization of these loop variables and setting up the corresponding Schrödinger equation are not clear [23]. We now briefly review the various operators in the Kogut-Susskind formulation [5] and define the prepotential operators [9] which enable us to solve the Mandelstam constraints exactly and explicitly in arbitrary dimensions.

2.2 The prepotential operators

The kinematical variables involved in Kogut and Susskind Hamiltonian formulation [5] of lattice gauge theories describe SU(2) rigid rotators attached to every link (n, i) of the lattice. The kinematical

[3]In [6] it is shown that the Mandelstam constraints constitute sufficient algebraic conditions on Wilson loop variables to allow reconstruction of the corresponding gauge potentials.

variables are: a) SU(2) link operators $U(n,i) = \begin{pmatrix} U_{11}(n,i) & U_{12}(n,i) \\ U_{21}(n,i) & U_{22}(n,i) \end{pmatrix}$, describing the orientation of the body fixed frame of the rigid body from the space fixed frame, b) the electric fields $E^a_L(n,i)$ and $E^a_R(n+i,i)$ which are the components of the angular momentum in the body fixed and space fixed frames respectively. This description is shown in Figure (2a). The link operators $U(n,i)$ satisfy the SU(2) conditions:

$$U(n,i)U^\dagger(n,i) = U^\dagger(n,i)U(n,i) = \mathcal{I}, \quad |U(n,i)| = 1. \tag{6}$$

Above $\mathcal{I}$ is 2×2 identity matrix and $|U| \equiv \det U$. The rigid body commutation relations are[4] [5]:

$$\begin{aligned} [E^a_L(n,i), U(n,i)] = -\left(\frac{\sigma^a}{2}\right) U(n,i) \quad &\Rightarrow \quad \left[E^a_L(n,i), E^b_L(n,i)\right] = i\epsilon^{abc}E^c_L(n,i), \\ [E^a_R(n+i,i), U(n,i)] = U(n,i)\left(\frac{\sigma^a}{2}\right) \quad &\Rightarrow \quad \left[E^a_R(n,i), E^b_R(n,i)\right] \;=\; i\epsilon^{abc}E^c_R(n,i) \end{aligned} \tag{7}$$

In (7), σ^a (a=1,2,3) are the Pauli matrices and the operators on different links commute. The angular momentum algebras on the r.h.s. of (7) follows from the Jacobi identities: $\left[E^a_{L(R)}, \left[E^b_{L(R)}, U_{\alpha\beta}\right]\right]$ + cyclic permutations $\equiv 0$. The link operators commute amongst themselves: $[U_{\alpha\beta}(n,i), U_{\gamma\delta}(m,j)] = \left[U_{\alpha\beta}(n,i), U^\dagger_{\gamma\delta}(m,j)\right] = 0$. Further, $E^a_L(n,i)$ and $E^a_R(n+i,i)$, being the body, space fixed components of the angular momentum operator of the rigid rotator on the link (n,i), mutually commute $\left[E^a_L(n,i), E^b_R(n+i,i)\right] = 0$. For the same reason, they satisfy the kinematical constraint:

$$\sum_{a=1}^{3} E^a_L(n,i)E^a_L(n,i) = \sum_{a=1}^{3} E^a_R(n+i,i)E^a_R(n+i,i) \equiv E^2(n,i), \quad \forall(n,i) \tag{8}$$

ensuring that their magnitudes are equal. The SU(2) gauge transformations correspond to separately rotating the body, space fixed frames of the rigid rotator [5]:

$$E_{L(R)}(n,i) \to \Lambda(n)E_{L(R)}(n,i)\Lambda^\dagger(n), \qquad U(n,i) \to \Lambda(n)U(n,i)\Lambda^\dagger(n+i). \tag{9}$$

In (9), $E_{L(R)} \equiv \sum_{a=1}^{3} E^a_{L(R)}\sigma^a$ and $\Lambda(n)$ is rotation matrix in the fundamental representation of SU(2) at lattice site n. The commutation relations (7) along with the gauge transformations (9) imply that the generators of SU(2) gauge transformations at any lattice site n are:

$$\mathcal{C}^a(n) = \sum_{i=1}^{3} \left(E^a_L(n,i) + E^a_R(n,i)\right), \quad \forall n, a. \tag{10}$$

The corresponding Gauss law constraints are $\mathcal{C}^a(n) = 0$. The commutation relations (7) and the constraints (8) imply that a complete set of commuting observables on every link (n,i) are: $E^2(n,i), E^z_L(n,i)$, $E^z_R(n+i,i)$ where $E^z_{L(R)}(n,i) \equiv E^{a=3}_{L(R)}(n,i)$ are the third components of the angular momenta. The corresponding orthonormal basis is denoted by $|j(n,i), m(n,i), \tilde{m}(n+i,i)\rangle$ where $j(n,i)$, $m(n,i)$, and $\tilde{m}(n+i,i)$ are the eigenvalues of the above 3 mutually commuting operators respectively. We now define the prepotential operators through the Jordan-Schwinger representation of the angular momentum algebra [17]:

$$E^a_L(n,i) \equiv \frac{1}{2}a^\dagger(n,i)\sigma^a a(n,i), \qquad E^a_R(n,i) \equiv \frac{1}{2}b^\dagger(n,i)\sigma^a b(n,i). \tag{11}$$

[4] In [9], we had used $E^a(n,i) = -E^a_L(n,i)$ and $e^a(n,i) \equiv E^a_R(n+i,i)$ resulting in an extra -ve signs in the commutation relations involving E^a_L in (7).

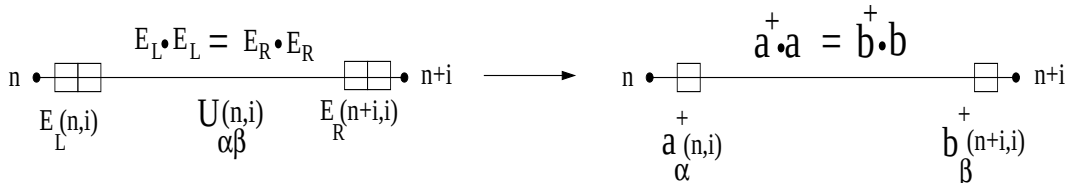

Figure 2: (a) The original $(E^a_L(n,i), E^a_R(n+i,i), U_{\alpha\beta}(n,i))$ operators, (b) the new $(a_\alpha(n,i), b_\alpha(n+i,i))$ operators on the link (n,i). The electric fields E_L, E_R transform in the adjoint representation. The prepotentials $a_\alpha(n,i), b_\alpha(n+i,i)$ transform as SU(2) fundamental doublets at lattice site n and n+i respectively. Therefore, we represent them by Young tableau $\square$ at n and n+i respectively.

The mapping (11) corresponds to associating two doublets of harmonic oscillator prepotentials $a^\dagger_\alpha(n,i)$ and $b^\dagger_\alpha(n+i,i)$ and their conjugates to the initial and the end points of the link (n,i) respectively. This assignment is shown in Figure (2b). The canonical electric field or angular momentum commutation relations in (7) are satisfied provided the prepotentials on every link (n,i) satisfy the standard harmonic oscillator algebra:

$$\left[a_\alpha, a^\dagger_\beta\right] = \delta_{\alpha\beta}, \qquad \left[b_\alpha, b^\dagger_\beta\right] = \delta_{\alpha\beta}, \qquad [a_\alpha, a_\beta] = 0, \qquad [b_\alpha, b_\beta] = 0. \tag{12}$$

The body and space fixed components of the angular momentum or electric fields mutually commute implying: $[a_\alpha, b^\dagger_\beta] = [a_\alpha, b_\beta] = 0$. Note that the prepotential vacuum state $|0\rangle$ on the link (n,i) satisfying: $a_\alpha(n,i)|0\rangle = 0,\ b_\alpha(n,i)|0\rangle = 0$ is the strong coupling vacuum defined as: $E^a_L(n,i)|0\rangle = 0,\ E^a_R(n,i)|0\rangle = 0$. In [24] anti-commuting oscillators, instead of (12), are used in (11) to treat QCD as quantum link models. We define the total number operators:

$$N_a(n,i) = a^\dagger(n,i)\cdot a(n,i), \qquad N_b(n,i) = b^\dagger(n,i)\cdot b(n,i),$$

where $a^\dagger\cdot a \equiv \sum_{\alpha=1}^{2} a^\dagger_\alpha a_\alpha$. The left and right Casimirs are: $E_L\cdot E_L \equiv \sum_{a=1}^{3} E^a_L E^a_L = N_a/2\,(N_a/2+1)$, $E_R\cdot E_R = N_b/2\,(N_b/2+1)$. Therefore, the kinematical constraints (8) in terms of the prepotentials mean that on every link (n,i), the number of left oscillators is equal to the number of right oscillator:

$$N_a(n,i) = N_b(n+i,i) \equiv N(n,i) \tag{13}$$

as shown in Figure (2b). Under SU(2) gauge transformations (9) at site n, the defining equations (11) imply that the prepotentials transform as SU(2) fundamental doublets:

$$a_\alpha(n,i) \to \Lambda_{\alpha\beta}(n) a_\beta(n,i), \qquad b_\alpha(n,i) \to \Lambda_{\alpha\beta}(n) b_\beta(n,i). \tag{14}$$

Therefore, unlike the link operators $U_{\alpha\beta}(n,i)$ transforming at both the ends of the link by $\Lambda(n)$ and $\Lambda(n+i)$ in (9), the prepotentials $(a_\alpha(n,i), b_\alpha(n,i))$ transform only at a single end by $\Lambda(n)$. In the next section this simple fact will enable us to define SU(2) invariant Hilbert spaces $\mathcal{H}^{SU(2)}(n)$ locally at every lattice site n.

In terms of the prepotential operators we have additional U(1) gauge invariance as their defining equations (11) are invariant under:

$$a^\dagger_\alpha(n,i) \to \lambda(n,i)\ a^\dagger_\alpha(n,i); \quad b^\dagger_\alpha(n+i,i) \to \lambda^\dagger(n,i)\ b^\dagger_\alpha(n+i,i). \tag{15}$$

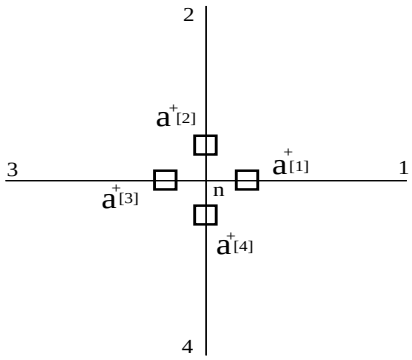

Figure 3: The 2d prepotential SU(2) doublets $a^\dagger[n,i]$, i=1,2,...,2d around every lattice site n shown in d = 2 by their Young tableau boxes □. They all transform as doublets under SU(2) gauge transformation at site n.

In (15), $\lambda(n,i) = expi\theta(n,i)$ is the abelian phase factor on the link (n,i). Note that the abelian transformations (15) leave the Hilbert space of the rigid rotators, satisfying the constraints (13), unchanged. The creation operators $a^\dagger_\alpha(n,i)$ and $b^\dagger_\beta(n+i,i)$ create and absorb unit abelian flux at lattice sites n and n+i on the link (n,i) respectively. Thus the operators $a^\dagger_\alpha(n,i)b^\dagger_\beta(n+i,i)$, $a_\alpha(n,i)b_\beta(n+i,i)$ create and annihilate an abelian flux line on the link (n,i) respectively. To analyze nonabelian SU(2) fluxes in terms of the prepotential operators, we consider the following commutation relations:

$$\left[E^a_L, a^\dagger_\alpha\right] = \frac{1}{2}a^\dagger_\beta\sigma^a_{\beta\alpha}, \qquad \left[E^a_R, b^\dagger_\alpha\right] = \frac{1}{2}b^\dagger_\beta\sigma^a_{\beta\alpha}.$$

The above relations imply that $a^\dagger_\alpha(n,i)b^\dagger_\beta(n,i)$ and $a_\alpha(n,i)b_\beta(n,i)$ on a link (n,i), like the the link operators $U_{\alpha\beta}(n,i)$, change the angular momentum $j(n,i)$ by $\pm\frac{1}{2}$. As an example the prepotential operators acting on the vacuum with $j=0$ create $j=\frac{1}{2}$ state: $(E_L\cdot E_L)\left[a^\dagger_\alpha|0\rangle\right] = \frac{3}{4}\left[a^\dagger_\alpha|0\rangle\right]$, $(E_R\cdot E_R)\left[b^\dagger_\alpha|0\rangle\right] = \frac{3}{4}\left[b^\dagger_\alpha|0\rangle\right]$. These results correspond to $(E_L\cdot E_L)\left[U_{\alpha\beta}|0\rangle\right] = \frac{3}{4}\left[U_{\alpha\beta}|0\rangle\right]$ and $(E_R\cdot E_R)\left[U_{\alpha\beta}|0\rangle\right] = \frac{3}{4}\left[U_{\alpha\beta}|0\rangle\right]$. More precisely, using the Wigner-Eckart theorem, the link operator can also be represented in terms of the prepotential operators [9]:

$$U_{\alpha\beta}(n,i) = F(n,i)\big(\tilde{a}^\dagger_\alpha(n,i)b^\dagger_\beta(n+i,i) + a_\alpha(n,i)\tilde{b}_\beta(n+i,i)\big)F(n,i). \tag{16}$$

In (16), $F(n,i)\equiv\left(N(n,i)+1\right)^{-\frac{1}{2}}$ is the normalization factor where $N(n,i)$ is defined in (13). Note that the r.h.s. of (16) is U(1) invariant and also has the required SU(2) gauge transformation property of $U(n,i)$ given in (9). Acting on the Hilbert space satisfying (13), the relation (16) is consistent with (6), (7) and $[U_{\alpha\beta}, U_{\gamma\delta}] = [U_{\alpha\beta}, U^\dagger_{\gamma\delta}] = 0$. The relations (11) and (16) provide complete mapping from the original operators satisfying (7) and the constraints (8) to the harmonic oscillator prepotential operators satisfying (12) and the constraints (13) respectively. For later convenience, we define the following π operation on every link:

$$\tilde{a}^\dagger_\alpha(n,i) \stackrel{\pi}{\rightarrow} a_\alpha(n,i), \qquad b^\dagger_\alpha(n,i) \stackrel{\pi}{\rightarrow} \tilde{b}_\alpha(n,i) \tag{17}$$

The link operator can now be written as $U_{\alpha\beta}(n,i) = F(n,i)\left(\tilde{a}^\dagger_\alpha(n,i)b^\dagger_\beta(n+i,i) + \pi(n,i)\right)F(n,i)$.

2.3 Non-abelian intertwining, abelian weaving and loop states

The advantage of the prepotential operators is that under SU(2) gauge transformations they transform locally as SU(2) fundamental doublets (14). Therefore, the SU(2) invariant loop Hilbert space $\mathcal{H}^L$ can be constructed and analyzed *locally* in terms of $\mathcal{H}^{SU(2)}(n)$ at different lattice sites n. In the next section this simple fact, in turn, will enable us to solve the Mandelstam constraints exactly. To appreciate and elaborate on these statements further, it is convenient to relabel all the prepotentials and the corresponding electric fields around a lattice site n. We define[5]: $a^\dagger_\alpha[n,i],\ i=1,2,...,2d$ where $a^\dagger_\alpha[n,i] \equiv a^\dagger_\alpha(n,i),\ a^\dagger_\alpha[n,d+i] \equiv b^\dagger_\alpha(n,i), i=1,2,..,d$ as shown in Figure (3). Thus, instead of the original $[E^a_L(n,i), E^a_R(n,i), U_{\alpha\beta}(n,i)]$ description, we now have $2d$ SU(2) doublet prepotential operators around every lattice site n as shown in Figure (3). The SU(2) gauge transformation:

$$a^\dagger_\alpha[n,i] \rightarrow a^\dagger_\beta[n,i]\Lambda^\dagger_{\beta\alpha}(n), \quad i=1,2,..,2d.$$

is represented in Figure (3) by a single Young tableau box on the link $[n,i]$ with $i=1,2,..2d$. Further defining $J^a[n,i] = a^\dagger[n,i]\frac{\sigma^a}{2}a[n,i]$, we get:

$$J^a[n,i] = E^a_L(n,i); \quad J^a[n,d+i] = E^a_R(n,i); \quad i=1,2,...,d. \tag{18}$$

Therefore, all possible SU(2) invariant operators at site n are given by "intertwining" (anti-symmetrizing) any two different prepotential SU(2) doublets:

$$L_{ij}(n) = \epsilon_{\alpha\beta}\ a^\dagger_\alpha[n,i]\ a^\dagger_\beta[n,j] \equiv a^\dagger[n,i]\cdot\tilde{a}^\dagger[n,j], \qquad i,j=1,2,...,2d; \quad i<j. \tag{19}$$

In (19), $\epsilon_{\alpha\beta}$ is completely antisymmetric tensor ($\epsilon_{11}=\epsilon_{22}=0, \epsilon_{12}=-\epsilon_{21}=1$) and $\tilde{a}^\dagger_\alpha \equiv \epsilon_{\alpha\beta}a^\dagger_\beta$. The $d(2d-1)$ intertwining operators $L_{ij}(n)$ in (19) correspond to putting the Young boxes in $[i]$ and $[j]$ directions vertically to construct SU(2) singlets. In Figure (4), we graphically show this by joining these boxes with thick lines. These intertwining operators along with $a^\dagger[n,i]\cdot a[n,j]$ are the basic SU(2) invariant operators. Any gauge invariant operator can be analyzed *locally* in terms of them[6]. Further, the $d(2d-1)$ operators $L_{ij}(n)$ at lattice site n play the role of "SU(2) gauge invariant bricks" which acting on the strong coupling vacuum create the complete SU(2) gauge invariant Hilbert space $\mathcal{H}^{SU(2)}(n)$ at n. Note that $L_{ij}(n) = -L_{ji}(n)$, $L_{ii}=0$ implying self intertwining is not allowed. Thus a basis in $\mathcal{H}^{\mathrm{SU(2)}}(n)$ is given by:

$$|\vec{l}(n)\rangle \equiv \left| \begin{array}{ccccccc} l_{12} & l_{13} & l_{14} & & .... & & l_{1(2d)} \\ & l_{23} & l_{24} & & .... & & l_{2(2d)} \\ & & .... & & .... & & .... \\ & & & l_{2d-2(2d-1)} & & l_{2d-2(2d)} & \\ & & & & & l_{2d-1(2d)} & \end{array} \right\rangle = \prod_{\substack{i,j=1 \\ j\rangle i}}^{2d} (L_{ij}(n))^{l_{ij}(n)}\,|0\rangle, \quad l_{ij}(n) \in \mathcal{Z}_+. \tag{20}$$

In (20), $\mathcal{Z}_+$ denotes the set of all non-negative integers and $l_{ij} (\equiv l_{ji}, l_{ii}=0)$ are $d(2d-1)$ SU(2) gauge invariant intertwining integer quantum numbers characterizing the SU(2) gauge invariant Hilbert space at the site n. These SU(2) singlet states can also be graphically represented by first assigning $l_{ij}(n)$ Young tableau boxes individually to the links $[n,i]$ and $[n,j]$ and then joining (intertwining) them

[5] Unless stated explicitly, the direction indices $[i],[j]$.. within square brackets will vary from 1 to 2d.

[6] See section 3 and appendix B for an explicit analysis of $TrU_{\mathrm{plaquette}}$.

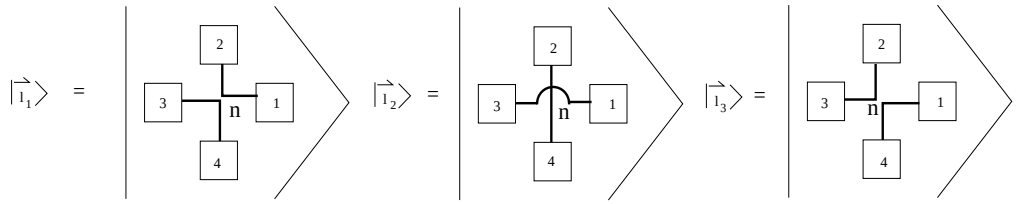

Figure 4: Graphical representation of SU(2) invariant intertwining illustrated for the states $|\vec{l_1}\ \rangle, |\vec{l_2}\ \rangle$ and $|\vec{l_3}\ \rangle$. The constraint $|\vec{l_1}\ \rangle = |\vec{l_2}\ \rangle - |\vec{l_3}\ \rangle$ at lattice site n represent the Mandelstam constraint in Figure (2) in terms of the prepotentials. The thick lines should be compared with the corresponding thick lines in Figure (1).

together. In Figure (4) we illustrate this graphical representation for the simple case involving the following three vectors in $d = 2$:

$$|\vec{l_1}\ \rangle = \left| \begin{array}{ccc} 1 & 0 & 0 \\ & 0 & 0 \\ & & 1 \end{array} \right\rangle, \quad |\vec{l_2}\ \rangle = \left| \begin{array}{ccc} 0 & 1 & 0 \\ & 0 & 1 \\ & & 0 \end{array} \right\rangle, \quad |\vec{l_3}\ \rangle = \left| \begin{array}{ccc} 0 & 0 & 1 \\ & 1 & 0 \\ & & 0 \end{array} \right\rangle \tag{21}$$

The above three states $|\vec{l_1}\ \rangle = L_{12}L_{34}|0\rangle,\ |\vec{l_2}\ \rangle = L_{13}L_{24}|0\rangle,\ |\vec{l_3}\ \rangle = L_{14}L_{23}|0\rangle$ are manifestly invariant under SU(2) gauge transformation. More explicitly, $|\vec{l}(n)\ \rangle$ in (20) satisfy the SU(2) Gauss law (10) constraints:

$$\mathcal{C}^a(n)|\vec{l}(n)\ \rangle = \sum_{i=1}^{2d} J^a[n,i]|\vec{l}(n)\ \rangle = J^a_{total}|\vec{l}(n)\ \rangle = 0 \tag{22}$$

as $[\mathcal{C}^a(n), L_{ij}(n)] = 0$ and $\mathcal{C}^a(n)|0\rangle = 0$. Thus all the states $|\vec{l}(n)\ \rangle$ in (20) at site n are the eigenstates of the total angular momentum at n with eigenvalues zero. Infact, the states $|\vec{l}(n)\ \rangle$ are also eigenstates of individual $2d$ Casimirs in (18):

$$J[n,i].J[n,i]|\vec{l}(n)\ \rangle = j[n,i](j[n,i]+1)|\vec{l}(n)\ \rangle, \quad i = 1,2,3,4 \tag{23}$$

where,

$$2j[n,i] = \sum_{k\neq i=1}^{2d} l_{ik}(n), \quad l_{ik}(n) = l_{ki}(n), \quad l_{ik}(n) \in \mathcal{Z}_+ \tag{24}$$

We note that (24) is both necessary and sufficient condition on $j[n,i], i = 1,2,3,..,2d$ to get SU(2) singlets.

Having solved the SU(2) Gauss law, we now focus on the abelian gauge transformations (15). As shown in Figure (2b), the abelian Gauss law (13) states that on any link the number of **a** type oscillators at the left end is equal to the number of **b** type oscillators at the right end. This can again be easily satisfied by putting $N_a(n,i) = N_b(n,i) = N(n,i)$ abelian flux lines on every link (n,i). Therefore, geometrically, the $SU(2) \otimes U(1)$ Gauss law demands the continuity of these U(1) flux lines on the entire lattice through SU(2) intertwining at every lattice site. In other words, all possible SU(2) invariant intertwining within $\mathcal{H}^{\mathrm{SU(2)}}(n)$ and U(1) weaving of the neighboring $\mathcal{H}^{\mathrm{SU(2)}}(n)$ is geometrically

equivalent to drawing all possible loops on the lattice leading to the loop Hilbert space $\mathcal{H}^L$. Given a configuration of closed loops on a lattice one can read off all the intertwining quantum numbers $l_{ij}(n)$ at site n by simply counting the number of loop lines going from $[i]^{th}$ to $[j]^{th}$ direction. The number of loops passing through a link $(n,i) = N_a(n,i) = 2j(n,i) = N_b(n+i,i)$ where $2j(n,i)$ is given in (24). The reverse is also true: given $l_{ij}(n)\ \forall\ n$, which are consistent with the U(1) gauge invariance, one can always draw corresponding closed loops. We now review the Mandelstam constraints in the basis (20) before solving them explicitly in terms of the prepotential operators.

2.3.1 Mandelstam constraints revisited

The basis $|\vec{l}(n)\ \rangle$ in (20) provides the local description of the Wilson loop basis in terms of the intertwining operators and intertwining quantum numbers at lattice site n. To see this explicitly, one writes Wilson loop operator Tr U_γ corresponding to a loop γ in terms of the prepotential operators using (16). It is clear that acting on the strong coupling vacuum they will produce states of the form $|\vec{l}(n)\ \rangle$ at every lattice site traversed by the loop γ. Thus, following the notation of section (2.1), the the Wilson loop basis can be locally characterized by $\mathcal{M}/n^d =$ (Number of intertwining quantum numbers per site $-$ Number of U(1) constraints per site) $= d(2d-1) - d = 2d(d-1)$ integers per lattice site. This establishes that the basis $|\vec{l}(n)\ \rangle$ describing the Wilson loop basis locally in terms of intertwining quantum numbers is over-complete. To illustrate this further and more explicitly, we again consider the vectors $|\vec{l_1}\ \rangle,\ |\vec{l_2}\ \rangle,\ |\vec{l_3}\ \rangle$ in (21) and shown in Figure (4). Using the identity:

$$(a^\dagger \cdot \tilde{b}^\dagger)(c^\dagger \cdot \tilde{d}^\dagger) \equiv (a^\dagger \cdot \tilde{c}^\dagger)(b^\dagger \cdot \tilde{d}^\dagger) - (a^\dagger \cdot \tilde{d}^\dagger)(b^\dagger \cdot \tilde{c}^\dagger), \tag{25}$$

we find the vectors in (21) are linearly dependent:

$$|\vec{l_1}\ \rangle = |\vec{l_2}\ \rangle\ -\ |\vec{l_3}\ \rangle \tag{26}$$

Infact, the SU(2) identity (2) involving link operators corresponds to the identity (25) and the Mandelstam constraint (4) is the constraint (26) written in terms of the relevant prepotential operators at site n. This can again be seen by writing the Mandelstam identity (2) in terms of prepotentials using (16) or comparing Figure (1a), (1b) and (1c) with Figure (4a), (4b) and (4c) respectively. In the prepotential language, the identities of the form (25) and their various powers will make the $|\vec{l}\ \rangle$ basis in (20) linearly dependent. Infact, this is what was done in (5) to get all the loop states on the two plaquettes related by Mandelstam constraints. Thus, at this stage, the problem of over-completeness of the Wilson loop basis can be analyzed locally in terms of the prepotentials.

2.3.2 The solutions

To solve the Mandelstam constraints we now need to focus only on a single lattice site[7] n. As discussed in section (2.2), the initial complete set of commuting observables at n consists of $4d$ angular momentum

[7]From now onwards we will be working locally at a given lattice site. Therefore, we will ignore the site index unless necessary. Also, we use the notation: $J_i^2 \equiv \sum_{a=1}^{3} J^a[n,i]J^a[n,i], i = 1,2...,2d$, the eigenvalues of J_i^2 are denoted by $j_i(j_i+1)$.

operators: $J_i^2, J_i^z, i = 1, 2, .., 2d$. Instead, we can also consider an equivalent basis where the following 4d mutually commuting operators [11, 12] are diagonal:

$$CSCO \equiv \left[J_1^2, ...J_{2d}^2; \left(J_1 + J_2\right)^2, \left(J_1 + J_2 + J_3\right)^2 ..., \left(J_1 + J_2 + J_3 ..... J_{(2d-1)}\right)^2, J_{total}^2, J_{total}^z\right] \quad (27)$$

where $J_{total}^2 = \left(J_1 + J_2^2 + J_3 ..... + J_{2d}\right)^2$ and $J_{total}^z = \left(J_1^{a=3} + J_2^{a=3} + J_3^{a=3} ..... + J_{2d}^{a=3}\right)$. The SU(2) Gauss law (22) demands $J_{total}^2 = J_{total}^z = 0$. Therefore, we drop the last two total angular momentum operators from the list (27). For later analysis, it is convenient to divide the remaining $(4d-2)$ operators in $CSCO$ (27) into two parts:

$$CSCO(I) = \left[J_1^2, J_2^2, .., J_{2d}^2\right], \quad CSCO(II) = \left[\left(J_1 + J_2\right)^2, ..., \left(J_1 + J_2 + J_3 ..... J_{(2d-1)}\right)^2 = J_{2d}^2\right] \quad (28)$$

The CSCO(I) contains 2d angular momentum Casimir operators along the 2d directions and the CSCO(II) contains the remaining $(2d-2)$ Casimirs in the above chosen angular momentum addition scheme. On $\mathcal{H}^{SU(2)}(n)$ the last two operators in CSCO(II) are equal because of the SU(2) Gauss law (22). We can, therefore, denote the corresponding SU(2) gauge invariant orthonormal eigenvectors by [11, 12]

$$|j_1, j_2, ..j_{2d}; j_{12}, j_{123}, ..., j_{12..(2d-1)} = j_{2d}\rangle \equiv |j_1, j_2, j_{12}, j_3, j_{123}, ..., j_{2d-1}, j_{12..(2d-1)} = j_{2d}\rangle. \quad (29)$$

The states in (29) are characterized by maximum possible $(4d-3)$ "good quantum numbers" which can be simultaneously measured at every lattice site. The SU(2) gauge invariant states $|\vec{l}\,\rangle$ in (20) are already eigenstates of of CSCO(I) with eigenvalues $2j_i = \sum_{k=1}^{2d} l_{ik}$ (see (23)). Therefore, we can relabel them in terms of their angular momenta:

$$|\,\vec{l}\,\rangle \rightarrow |j_1, j_2, ..., j_{2d}, j_{total} = m_{total} = 0\rangle \quad (30)$$

We note that the mapping (30) is many to one or degenerate because of the following discrete symmetries of the angular momenta j_i (i=1,2,...,2d) in (24):

$$\begin{aligned} &l_{i_1 i_2} \rightarrow l_{i_1 i_2} + r + t, \quad l_{i_1 i_3} \rightarrow l_{i_1 i_3} - r + s, \quad l_{i_1 i_4} \rightarrow l_{i_1 i_4} - s - t, \\ &l_{i_2 i_3} \rightarrow l_{i_2 i_3} - s - t, \quad l_{i_2 i_4} \rightarrow l_{i_2 i_4} - r + s, \quad l_{i_3 i_4} \rightarrow l_{i_3 i_4} + r + t. \end{aligned} \quad (31)$$

In (31) $i_1 \neq i_2 \neq i_3 \neq i_4$ are any four different directions and r,s and t can take all possible $\pm$ integer values such that $l_{i,j} \geq 0$. The advantage of the mapping (30) is that the states in (20) with different $\vec{l}$ which are related by (31) are precisely the states related by the the Mandelstam constraints (25). In other words, the states related by Mandelstam constraints are degenerate with respect to CSCO(I). The reverse is also true: the degenerate states with respect to CSCO(I) are all related by the Mandelstam constraints (25). As an example, we again consider the three loop states in (21): $|\vec{l_1}\,\rangle, |\vec{l_2}\,\rangle$ and $|\vec{l_3}\,\rangle$ in d=2 which are related by the Mandelstam constraints (25). In terms of the angular momenta:

$$\left.\begin{array}{l} |\vec{l_1}\,\rangle \\ |\vec{l_2}\,\rangle \\ |\vec{l_3}\,\rangle \end{array}\right\} \rightarrow |j_{i_1} = j_{i_2} = j_{i_3} = j_{i_4} = \frac{1}{2}, j_{total} = m_{total} = 0\rangle.$$

Also, given $j_1 = j_2 = j_3 = j_4 = \frac{1}{2}$, the above three possible partitions $\{\vec{l_1}\}, \{\vec{l_2}\}$ and $\{\vec{l_3}\}$ given in (21), are mutually related by (31). Therefore, we can lift the degeneracy and solve the Mandelstam constraints by demanding that the CSCO(I) degenerate eigenbasis (20) to be the eigenstates of CSCO(II)

as well. We conclude that a complete orthonormal loop basis in d dimension is locally characterized by $(4d-3)$ angular momentum quantum numbers and are given in (29). Note that the $(2d-3)$ eigenvalues of CSCO(II) are not free and have to satisfy the triangular constraints:

$$|j_{12..(k-1)} - j_k| \leq j_{12..k} \leq j_{12..(k-1)} + j_k, \quad k = 2, 3, ..., (2d-1) \tag{32}$$

along with $j_{12..(2d-1)} = j_{2d}$.

2.3.3 Solving the triangular constraints

The above characterization of the physical Hilbert space in terms of the angular momentum quantum numbers has been given in the context of duality transformation in lattice gauge theories [11] leading to a description in terms of triangulated surfaces [12]. In this section, we further solve the triangular constraints, geometrically representing triangulated 2 dimensional surfaces, in terms of the intertwining quantum numbers $\{\vec{l}\}$ which geometrically represent one dimensional loops.

In terms of the prepotentials (see Figure (3)) the SU(2) invariant states $|j_1, j_2, ..., j_{2d}\rangle$ in the mapping (30) represent $\sum_k l_{ik} (= 2j_i)$ Young tableau boxes on the $[i]^{th}$ link. Let us first consider (12) plane. To get the state $|j_1, j_2, ..., j_{2d}; j_{12}\rangle$ from the degenerate state $|j_1, j_2, ..., j_{2d}\rangle$, we need to intertwine (antisymmetrize) l_{12} boxes from $2j_1$ boxes with l_{12} boxes from $2j_2$ boxes so that we are left with $2j_{12}$ boxes in the (12) plane. Therefore, $2j_{12} = 2j_1 + 2j_2 - 2l_{12}$. This process is sequential and can be repeated to get the eigenvalues of the CSCO(II) also in terms of the linking numbers:

$$\begin{aligned}
l_{12} &= j_1 + j_2 - j_{12} \\
l_{13} + l_{23} &= j_{12} + j_3 - j_{123} \\
l_{14} + l_{24} + l_{34} &= j_{123} + j_4 - j_{1234} \\
..... & ..... \\
l_{1(2d)} + l_{2(2d)} + ... + l_{1(2d)} &= j_{12...(2d-1)} (= j_{2d}) + j_{2d} - j_{12...(2d)} (= 0) = 2j_{2d}
\end{aligned} \tag{33}$$

Given j_{12} at a lattice site, the top equation fixes l_{12}, the next line fixes $l_{13} + l_{23}$ in terms of j_{12} and j_{123},....., the last equation in (33) is an identity as it is already contained in (24). In appendix A, a detailed technical calculation, involving properties of SU(2) coherent states, shows that the final orthonormal and manifestly SU(2) gauge invariant loop states $|LS\rangle_n$ spanning the Hilbert space $\mathcal{H}^{SU(2)}$(n) are:

$$|LS\rangle_n \equiv |j_1, j_2, ..j_{2d}; j_{12}, j_{123}, ...j_{12..(2d-1)} = j_{2d}\rangle = N(j) \sum_{\{l\}}{}' \prod_{\substack{i,j \\ i<j}} \frac{1}{l_{ij}!} \big(L_{ij}(n)\big)^{l_{ij}(n)} |0\rangle \tag{34}$$

The prime over the summation means that, the linking numbers l_{ij} are are summed over all possible values which are consistent with (24) and (33). *This summations corresponds to taking appropriate linear combination of the degenerate loop eigenstates of CSCO(I) related by the Mandelstam constraints to produce an orthonormal and complete basis.* The normalization constant in (34) is given by:

$$N(j) = N(j_1, j_2, j_{12}) N(j_{12}, j_3, j_{123}) N(j_{123}, j_4, j_{1234}) ..... N(j_{2d}, j_{2d}, 0) \tag{35}$$

where $N(a,b,c) = \left[\frac{(2c+1)}{(a+b+c+1)!}\right]^{\frac{1}{2}} \left[(-a+b+c)!(a-b+c)!(a+b-c)!\right]^{\frac{1}{2}}$. We emphasize that this simple construction (34) of the orthonormal loop basis in terms of intertwining operators L_{ij} and intertwining linking numbers l_{ij} in arbitrary dimensions becomes extremely involved and complicated in terms of the link operators $U_{\alpha\beta}$ and the angular momentum quantum numbers[8].

As an example, we again consider the states $|\vec{l_1}\,\rangle, |\vec{l_2}\,\rangle$ and $|\vec{l_3}\,\rangle$ and solve the Mandelstam constraint (26). Our result (34) immediately gives us the corresponding two independent (orthonormal) states:

$$\begin{aligned} |j_1 = j_2 = j_3 = j_4 = \frac{1}{2}, j_{12} = 0\rangle &= \frac{1}{2}|\vec{l_1}\rangle, \\ |j_1 = j_2 = j_3 = j_4 = \frac{1}{2}, j_{12} = 1\rangle &= \frac{1}{2\sqrt{3}}\left[|\vec{l_2}\rangle + |\vec{l_3}\rangle\right] \end{aligned} \tag{36}$$

It can be explicitly checked that the above two states are individually normalized and mutually orthogonal.

It is perhaps worth going back and also solve the Mandelstam constraints for the example given in section 2.1 with arbitrary N_A and N_B in 2 dimension. In this special case: $2j_1(n) = 2j_2(n) = N_A$ and $2j_3(n) = 2j_4(n) = N_B$. The single state shown in the top r.h.s. of (5) correspond to $l_{12} = N_A$ and hence $j_{12} = j_1 + j_2 - l_{12} = 0$ at site n. The two states in the second top line of (5) represent $l_{12}(n) = N_A - 1$ and therefore correspond to $j_{12}(n) = 1$, the three states in the next line have $l_{12}(n) = N_A - 2$ or equivalently $j_{12}(n) = 2$ and so on so forth. The $(N_{\min} + 1)$ states in the last line of (5) correspond to $l_{12}(n) = 0$ if $N_A < N_B$ and $l_{12}(n) = N_B$ if $N_B < N_A$. Therefore, these states at n correspond to $j_{12}(n) = 2j_1$ if $(N_A < N_B)$ and $j_{12} = 2(j_1 - j_2)$ if $(N_B < N_A)$. Using the relative weights in (34), one can easily construct an orthonormal basis in $\mathcal{H}^{\mathrm{SU(2)}}(\mathrm{n})$.

As mentioned before, the $SU(2) \otimes U(1)$ invariant orthonormal loop states on the lattice can be obtained by drawing all possible loops on the lattice and computing the $4d-3$ "good quantum numbers" in (29) and constructing (34) at every lattice site. All possible orthonormal loop states on lattice can be formally written as:

$$|LS\rangle_{\mathrm{lattice}} = \left(\prod_{(n,i)\in \mathrm{lattice}} \int_0^{2\pi} d\phi(n,i) exp\ i\ \phi(n,i)\,(j[n,i] - j[n+i,d+i])\right) \prod_{n\in \mathrm{lattice}} \otimes |LS\rangle_n \tag{37}$$

The auxiliary angular fields $\phi(n,i), 0 < \phi(n,i) \leq 2\pi$ in (37) on every link implement the U(1) Gauss law (13). Note that the U(1) Gauss law provides d relations per lattice site. Therefore, without any over counting, there are $\mathcal{N}/n^d = 4d - 3 - d = 3(d-1)$ "good quantum numbers" associated with the loop states per lattice site in the final construction (37). This was the desired number we started with right in the beginning (see equation (1)).

[8]The states $|j_1, j_2, j_{12}, j_3, j_{123}, ..., j_{2d-1}, j_{12..(2d-1)}, j_{total}, m_{total}\rangle$ can be obtained by using Clebsch-Gordan coefficients: $|j_1, j_2, j_{12}, j_3, j_{123}, ...j_{12..(2d-1)} = j_{2d}\rangle = \sum_{\vec{m}} C^{j_{12..2d}=0 m_{12..2d}=0}_{j_{12..(2d-1)} m_{12..(2d-1)}, j_{2d} m_{2d}} ..... C^{j_{123} m_{123}}_{j_{12} m_{12}, j_3 m_3} C^{j_{12} m_{12}}_{j_1 m_1, j_2 m_2} \prod_{i=1}^{2d} \otimes |j_i m_i\rangle$. However, such approaches lead to rapid proliferation of gauge non-invariant Clebsch Gordan coefficients [16] forcing one to use graphical methods to avoid this problem. In contrast, the construction (34) in terms of gauge invariant intertwining numbers (not angular momentum) is simple and bypasses this problem.

2.4 Matter, loops and strings

The inclusion of fundamental matter fields is also natural in the prepotential formulation. It simply increases the number of intertwining operators at every lattice site. For simplicity, we introduce scalar matter field operators: $(\phi_\alpha(n), \phi^*_\alpha(n))$ and their conjugate momenta $(\pi_\alpha(n), \pi^*_\alpha(n))$ respectively. They are neutral under U(1) gauge transformations and transform as doublets under SU(2) gauge transformations: $\phi_\alpha(n) \to \Lambda_{\alpha\beta}(n)\phi_\beta(n)$, $\pi^*_\alpha(n) \to \Lambda_{\alpha\beta}(n)\pi^*_\beta(n)$. The canonical commutation relations are:

$$\begin{aligned} [\pi_\alpha(n), \phi_\beta(m)] &= [\pi^*_\alpha(n), \phi^*_\alpha(n)] = -\, i\, \delta_{\alpha\beta}\delta_{nm}, \\ [\pi_\alpha(n), \pi_\beta(m)] &= [\phi_\alpha(n), \phi_\beta(m)] = 0, \\ \left[\pi_\alpha(n), \pi^*_\beta(m)\right] &= \left[\phi_\alpha(n), \phi^*_\beta(m)\right] = 0. \end{aligned} \tag{38}$$

The matter creation and annihilation operators are defined as:

$$\begin{aligned} \mathsf{a}^\dagger_\alpha(n) &\equiv \frac{1}{\sqrt{2}}\left[\pi_\alpha(n) + i\phi^*_\alpha(n)\right], \qquad \mathsf{a}_\alpha(n) \equiv \frac{1}{\sqrt{2}}\left[\pi^*_\alpha(n) - i\phi_\alpha(n)\right], \\ \mathsf{b}^\dagger_\alpha(n) &\equiv \frac{1}{\sqrt{2}}\left[\pi^*_\alpha(n) + i\phi_\alpha(n)\right], \qquad \mathsf{b}_\alpha(n) \equiv \frac{1}{\sqrt{2}}\left[\pi_\alpha(n) - i\phi^*_\alpha(n)\right]. \end{aligned} \tag{39}$$

Like the prepotential operators they satisfy:

$$\begin{aligned} \left[\mathsf{a}_\alpha(n), \mathsf{a}^\dagger_\beta(m)\right] &= 1, \qquad \left[\mathsf{b}_\alpha(n), \mathsf{b}^\dagger_\beta(m)\right] = 1, \\ \left[\mathsf{a}_\alpha(n), \mathsf{b}_\beta(m)\right] &= 0, \qquad \left[\mathsf{a}_\alpha(n), \mathsf{b}^\dagger_\beta(m)\right] = 0. \end{aligned} \tag{40}$$

Under SU(2):

$$\mathsf{a}_\alpha(n) \to \Lambda_{\alpha\beta}(n)\mathsf{a}_\beta(n), \qquad \mathsf{b}^\dagger_\alpha(n) \to \Lambda_{\alpha\beta}(n)\mathsf{b}^\dagger_\beta(n), \tag{41}$$

they transform exactly like prepotentials (14) thus putting matter and gauge sector on the same footing under non-abelian gauge transformations. Therefore, we now have to construct SU(2) singlets out of $(2d+2)$ types of SU(2) doublets of creation operators per lattice site instead of 2d types as in the case of pure gauge theory. The orthonormal SU(2) gauge invariant states are now characterized by:

$$|j_1, j_2, j_{12}, j_3, j_{123}, \ldots\ldots\ldots j_{12\ldots(2d-1)}, j_{2d}, j_{12\ldots 2d}, j_{(2d+1)}, j_{12\ldots(2d+1)} = j_{(2d+2)}\rangle. \tag{42}$$

Further, the iterative method in appendix A again goes through and the states (42) can be easily constructed in terms of intertwining operators which will now involve matter creation operators (39) also.

As the matter fields transform like SU(2) doublets and are neutral under U(1) gauge transformations, they provide end points for the abelian flux lines leading to a gauge invariant description of lattice gauge theories in terms of loops and strings. Note that including scalar matter in the fundamental representation amounts to $d \to d+1$. The extra quantum numbers required per lattice site due to the inclusion of matter is $[4(d+1)-3] - [4d-3] = 4$, as expected.

3 The dynamical issues

To discuss dynamics of loops, we consider pure SU(2) lattice gauge theory Hamiltonian [5]:

$$H = \frac{g^2}{2}\sum_{n,i} E^2(n,i) + \frac{2}{g^2}\sum_{\Box}(2 - \mathrm{Tr}U_{\Box}) \tag{43}$$

where,

$$U_{\Box} = U_{\text{plaquette}} = U(n,i)U(n+i,j)U^{\dagger}(n+j,i)U^{\dagger}(n,j), \tag{44}$$

g is the coupling constant and $E^2(n,i) = E_L^2(n,i) = E_R^2(n+i,i)$ (see (8)). The loop states discussed in section (2) trivially diagonalize the electric field term with eigenvalues $\sum_{loops} j(n,i)\,(j(n,i)+1)$ where $\sum_{loops}$ denotes summation over all the links on the loops. The electric field term in this loop basis is like potential energy term and counts the number of abelian flux lines on that link. The plaquette term acts like kinetic energy term: it makes the loops fluctuate over the corresponding plaquette by creating and destroying the abelian flux lines (16).

3.1 The loop dynamics

As mentioned in the introduction, we restrict ourselves to d=2 and generalize the results to arbitrary d dimension at the end. We consider a plaquette abcd as shown in the Figure (5) with the four edges $(\mathbf{ab}), (\mathbf{bc}), (\mathbf{cd}), (\mathbf{da})$ denoted by l_1, l_2, l_3, l_4 respectively. Using (16) and (17), we write the gauge invariant plaquette operator over *abcd* in terms of the prepotentials:

$$\mathrm{Tr}U_{abcd} = F_{abcd}\Big[\left(a^{\dagger}[1]\cdot\tilde{a}^{\dagger}[2]\right)_a\left(a^{\dagger}[2]\cdot\tilde{a}^{\dagger}[3]\right)_b\left(a^{\dagger}[3]\cdot\tilde{a}^{\dagger}[4]\right)_c\left(a^{\dagger}[4]\cdot\tilde{a}^{\dagger}[1]\right)_d + \sum_{i=1}^{4}\pi(l_i) +$$
$$\sum_{i,j>i=1}^{4}\pi(l_i)\pi(l_j) + \sum_{i,j>i,k>j=1}^{4}\pi(l_i)\pi(l_j)\pi(l_k) + \pi(l_1)\pi(l_2)\pi(l_3)\pi(l_4)\Big]F_{abcd} \equiv \sum_{\alpha\beta\gamma\delta=\pm} H_{\alpha\beta\gamma\delta} \tag{45}$$

where $F_{abcd} \equiv F(l_1)F(l_2)F(l_3)F(l_4)$. In (45), there are sixteen $SU(2)\otimes U(1)$ gauge invariant terms which are produced by substituting (16) in (44). The first plaquette operator on the r.h.s. of the top equation in (45) is written explicitly in terms of the prepotential intertwining operators at lattice

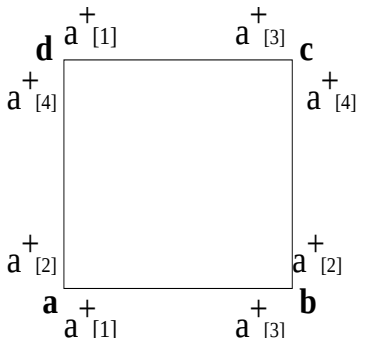

Figure 5: The plaquette **abcd** with the corresponding prepotential operators from Figure (3).

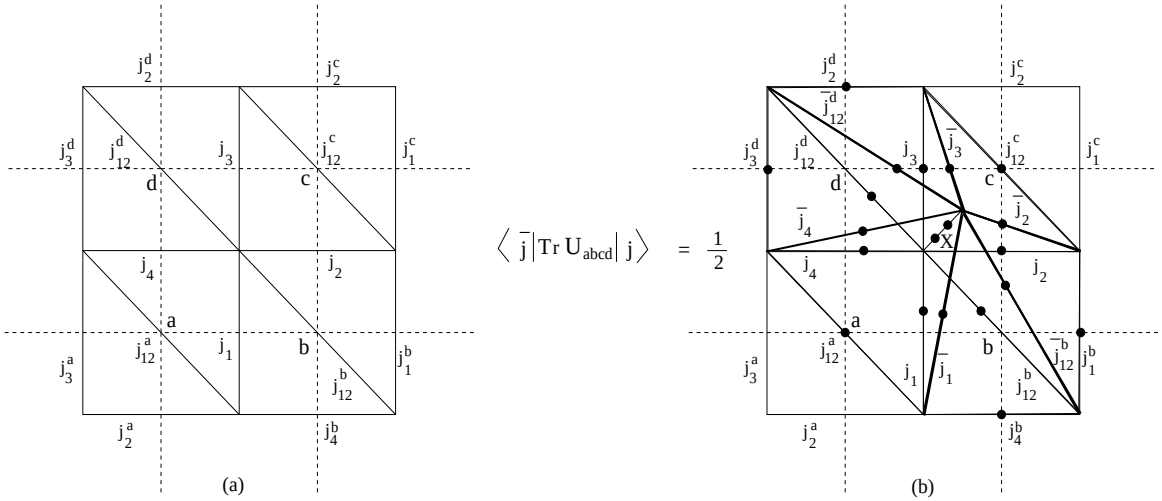

Figure 6: From loop kinematics to loop dynamics. (a) The angular momenta satisfying SU(2) Gauss law on the dual lattice, (b) The matrix elements $\langle \bar{j}_{abcd}|\mathrm{Tr}\, U_{abcd}|j_{abcd}\rangle$ with $X = \frac{1}{2}$ (also see [12]). The six tetrahedron are the six $6j$ symbols in (48). The unchanged j lines represent the delta function and a $\bullet$ over a j line represents the factor $(-1)^j \Pi(j)$ leading to $\mathcal{M}_{abcd}$ in (48).

sites **a**, **b**, **c** and **d** in Figure (5). It increases angular momenta by $\frac{1}{2}$ on the four links of *abcd* and therefore we represent it by H_{++++}. The rest of the 15 plaquette operators in (45) are generated by the action of π on it. The single π operation at any of the 4 links (l_1, l_2, l_3, l_4) acting on H_{++++} produces 4 terms: $H_{-+++}, H_{+-++}, H_{++-+}, H_{+++-}$. Similarly, the double π operation produces 6 operators: $H_{--++}, H_{-+-+}, H_{-++-}, H_{+--+}, H_{+-+-}, H_{++--}$. There are four 3 π terms in (45): $H_{+---}, H_{-+--}, H_{--+-}, H_{---+}$. Finally, the 4 π operation on all the four links produces a single term: H_{----}. Note that $\left(H_{\alpha\beta\gamma\delta}\right)^\dagger = H_{-\alpha-\beta-\gamma-\delta}$. The advantage of the form (45) is that now this magnetic field term can be analyzed locally at **a**, **b**, **c** and **d** in the manifestly SU(2) gauge invariant way. To compute the action of U_{abcd}, it is convenient to label the loop state (34) at abcd as $|j_{abcd}\rangle$:

$$|j_{abcd}\rangle \equiv |j_1^a j_2^a j_3^a j_4^a j_{12}^a\rangle \otimes |j_1^b j_2^b j_3^b j_4^b j_{12}^b\rangle \otimes |j_1^c j_2^c j_3^c j_4^c j_{12}^c\rangle \otimes |j_1^d j_2^d j_3^d j_4^d j_{12}^d\rangle. \tag{46}$$

The U(1) Gauss law demands:

$$j_1^a = j_3^b \equiv j_1,\ j_2^b = j_4^c \equiv j_2,\ j_3^c = j_1^d \equiv j_3,\ j_4^d = j_2^a \equiv j_4. \tag{47}$$

The matrix elements of $\mathrm{Tr}U_{abcd}$ are computed directly in the loop basis (46) in appendix B using generalized Wigner-Eckart theorem and Biedenharn-Elliot identities. The final result is:

$$\begin{aligned}\langle \bar{j}_{abcd}|\mathrm{Tr}U_{abcd}|j_{abcd}\rangle \;=\; \mathcal{M}_{abcd} &\begin{Bmatrix} j_1 & \bar{j}_1 & \frac{1}{2} \\ \bar{j}_4 & j_4 & j_{12}^a \end{Bmatrix}\begin{Bmatrix} j_{12}^b & \bar{j}_{12}^b & \frac{1}{2} \\ \bar{j}_1 & j_1 & j_4^b \end{Bmatrix}\begin{Bmatrix} j_{12}^b & \bar{j}_{12}^b & \frac{1}{2} \\ \bar{j}_2 & j_2 & j_1^b \end{Bmatrix} \\ &\begin{Bmatrix} j_3 & \bar{j}_3 & \frac{1}{2} \\ \bar{j}_2 & j_2 & j_{12}^c \end{Bmatrix}\begin{Bmatrix} j_{12}^d & \bar{j}_{12}^d & \frac{1}{2} \\ \bar{j}_3 & j_3 & j_2^d \end{Bmatrix}\begin{Bmatrix} j_{12}^d & \bar{j}_{12}^d & \frac{1}{2} \\ \bar{j}_4 & j_4 & j_3^d \end{Bmatrix}.\end{aligned} \tag{48}$$

In (48), $\mathcal{M}_{abcd} \equiv D_{abcd} N_{abcd} P_{abcd}$ where:

$$\begin{aligned} D_{abcd} &= \delta_{j_3^a,\bar{j}_3^a}\delta_{j_4^a,\bar{j}_4^a}\delta_{j_{12}^a,\bar{j}_{12}^a}\delta_{j_1^b,\bar{j}_1^b}\delta_{j_4^b,\bar{j}_4^b}\delta_{j_1^c,\bar{j}_1^c}\delta_{j_2^c,\bar{j}_2^c}\delta_{j_{12}^c,\bar{j}_{12}^c}\delta_{j_2^d,\bar{j}_2^d}\delta_{j_3^d,\bar{j}_3^d}, \\ N_{abcd} &= \Pi\left(j_1,\bar{j}_1,j_2,\bar{j}_2,j_3,\bar{j}_3,j_4,\bar{j}_4,j_{12}^b,\bar{j}_{12}^b,j_{12}^d,\bar{j}_{12}^d\right) \\ P_{abcd} &= -(-1)^{j_1+j_2+j_1^b+j_4^b}(-1)^{j_3+j_4+j_3^d+j_2^d}\triangle(\bar{j}_1,\bar{j}_4,j_{12}^a)\triangle(\bar{j}_2,\bar{j}_3,j_{12}^c)\triangle(\bar{j}_{12}^b,j_{12}^b,\frac{1}{2})\triangle(\bar{j}_{12}^d,j_{12}^d,\frac{1}{2}). \end{aligned} \tag{49}$$

In (49), D_{abcd} describes the trivial δ functions over the angular momenta which do not change under the action of the plaquette operator (45), N_{abcd} and P_{abcd} give the corresponding numerical and the phase factors respectively. The multiplicity factors are: $\Pi(x,y,...) \equiv \sqrt{(2x+1)(2y+1)...}$ and $\triangle(x,y,z)$ represent the phase factors associated with a triangle with sides x, y, z: $\triangle(x,y,z) \equiv (-1)^{x+y+z} \Rightarrow \triangle(x,y,z) = \pm 1$. The matrix elements (48) describe the dynamics in the loop basis (34) and can be geometrically represented by the Figure (6b). This dynamics contains three physical discrete angular momentum loop co-ordinates numbers per lattice site. The matrix elements (48) have been obtained[9] in the context of dual description [12, 14] of (2+1) dimension lattice gauge theory in terms of triangulated surfaces. It is easy to see that the matrix elements in (48) are symmetric: the 6j symbols satisfy $\left\{ \begin{array}{ccc} x & \bar{x} & u \\ \bar{y} & y & v \end{array} \right\} = \left\{ \begin{array}{ccc} \bar{x} & x & u \\ y & \bar{y} & v \end{array} \right\}$ and the factors D_{abcd}, N_{abcd} and P_{abcd} are individually symmetric under $j_{abcd} \leftrightarrow \bar{j}_{abcd}$. The matrix elements in (48) are also real as $\mathrm{Tr}U_{\mathrm{plaquette}}$ is a Hermitian operator. This reality can again be easily seen as the 6j symbols, $D_{abcd}, N_{abcd}, \triangle(abc)$ are themselves real. The remaining two phase factors $(-1)^{j_1+j_2+j_1^b+j_4^b}$ and $(-1)^{j_3+j_4+j_2^d+j_3^d}$ in P_{abcd} are real because (j_1, j_2, j_1^b, j_4^b) and (j_3, j_4, j_3^d, j_2^d) are the coordinates of the loop states at **b** and **d** respectively. Therefore, (24) implies: $j_1+j_2+j_1^b+j_4^b = Integer,\ j_3+j_4+j_2^d+j_3^d = Integer \Rightarrow P_{abcd} = \pm 1$. At this stage, before generalizing the loop dynamics to arbitrary d dimension, we cross check the d = 2 result (48). As the six 6j symbols and the δ functions in D_{abcd} are geometrical in origin, we only need to check the numerical and the phase factors $N_{abcd},\ P_{abcd}$ respectively. For this purpose, we replace $\mathrm{Tr}U_{abcd}$ by the identity operator $\mathcal{I}$. The computations in appendix B imply that now we only have to replace $\frac{1}{2}$ in each of the six 6j symbols in (48) and in P_{abcd} in (49) by 0. Using the value $\left\{ \begin{array}{ccc} a & \bar{a} & 0 \\ \bar{b} & b & d \end{array} \right\} = (-1)^{a+b+d}\delta_{a,\bar{a}}\delta_{b,\bar{b}}\left(\Pi(a,b)\right)^{-1}$, we get:

$$\left\{ \begin{array}{ccc} j_1 & \bar{j}_1 & 0 \\ \bar{j}_4 & j_4 & j_{12}^a \end{array} \right\}\left\{ \begin{array}{ccc} j_{12}^b & \bar{j}_{12}^b & 0 \\ \bar{j}_1 & j_1 & j_4^b \end{array} \right\}\left\{ \begin{array}{ccc} j_{12}^b & \bar{j}_{12}^b & 0 \\ \bar{j}_2 & j_2 & j_1^b \end{array} \right\} \left\{ \begin{array}{ccc} j_3 & \bar{j}_3 & 0 \\ \bar{j}_2 & j_2 & j_{12}^c \end{array} \right\}\left\{ \begin{array}{ccc} j_{12}^d & \bar{j}_{12}^d & 0 \\ \bar{j}_3 & j_3 & j_2^d \end{array} \right\}\left\{ \begin{array}{ccc} j_{12}^d & \bar{j}_{12}^d & 0 \\ \bar{j}_4 & j_4 & j_3^d \end{array} \right\} = \frac{\delta_{j_1,\bar{j}_1}\delta_{j_2,\bar{j}_2}\delta_{j_3,\bar{j}_3}\delta_{j_4,\bar{j}_4}\delta_{j_{12}^b,\bar{j}_{12}^b}\delta_{j_{12}^d,\bar{j}_{12}^d}}{N_{abcd}\ P_{abcd}}, \tag{50}$$

Geometrically, the equation (50) corresponds to putting $X = 0$ in the Figure (6b). It implies $\langle \bar{j}_{abcd}|\mathcal{I}|j_{abcd}\rangle = \delta_{\bar{j}_{abcd},j_{abcd}}$ confirming the numerical and the phase factors in (48). We now write (48) in a more compact form which can be directly generalized to higher dimension. Henceforth, we

[9] Our phase factors in (49) are different resulting in real and symmetric matrix $\langle \bar{j}_{abcd}|\mathrm{Tr}U_{abcd}|j_{abcd}\rangle$ in (48).

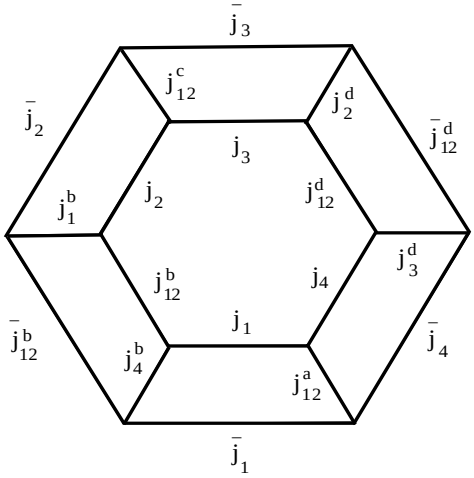

Figure 7: The $18j$ ribbon diagram representing exact SU(2) loop dynamics without any spurious gauge or loop degrees of freedom in d=2. The interior (exterior) edge carries the initial (final) angular momenta and the six bridges carry the angular momenta which are invariant under the action of $\mathrm{Tr}U_{\square}$. The six bridges along with the respective four angular momenta attached represent the six $6j$ symbols appearing in (51) with $\bar{j}_i = j_i \pm \frac{1}{2}$.

ignore D_{abcd} representing trivial δ functions in (48). We write:

$$\langle \bar{j}_{abcd}|\mathrm{Tr}U_{abcd}|j_{abcd}\rangle = N_{abcd}\sum_x (2x+1)(-1)^{r+2x} \left\{ \begin{array}{ccc} j_1 & \bar{j}_1 & x \\ \bar{j}_4 & j_4 & j^a_{12} \end{array} \right\} \left\{ \begin{array}{ccc} \bar{j}_4 & j_4 & x \\ j^d_{12} & \bar{j}^d_{12} & j^d_3 \end{array} \right\}$$

$$\left\{ \begin{array}{ccc} j^d_{12} & \bar{j}^d_{12} & x \\ \bar{j}_3 & j_3 & j^d_2 \end{array} \right\} \left\{ \begin{array}{ccc} \bar{j}_3 & j_3 & x \\ j_2 & \bar{j}_2 & j^c_{12} \end{array} \right\} \left\{ \begin{array}{ccc} j_2 & \bar{j}_2 & x \\ \bar{j}^b_{12} & j^b_{12} & j^b_1 \end{array} \right\} \left\{ \begin{array}{ccc} \bar{j}^b_{12} & j^b_{12} & x \\ j_1 & \bar{j}_1 & j^b_4 \end{array} \right\} \prod_{i=1}^{4} \left(\delta_{\bar{j}_i, j_i+\frac{1}{2}} + \delta_{\bar{j}_i, j_i-\frac{1}{2}} \right)$$

$$= N_{abcd} \underbrace{\left[\begin{array}{cccccccccccc} j_1 & & j_4 & & j^d_{12} & & j_3 & & j_2 & & j^b_{12} & \\ & j^a_{12} & & j^d_3 & & j^d_2 & & j^c_{12} & & j^b_1 & & j^b_4 \\ \bar{j}_1 & & \bar{j}_4 & & \bar{j}^d_{12} & & \bar{j}_3 & & \bar{j}_2 & & \bar{j}^b_{12} & \end{array} \right]}_{\text{18j coefficient of the second kind}} \prod_{i=1}^{4} \left(\delta_{\bar{j}_i, j_i+\frac{1}{2}} + \delta_{\bar{j}_i, j_i-\frac{1}{2}} \right) \quad (51)$$

The 18j symbols in (51) are shown in (7). Note that $P_{abcd}\left(=(-1)^{r+1}\right)$ in (49) is precisely the phase factor needed to define 18j symbol [26] in (51). Further, the 12 triangular constraints in (51) at the 12 vertices of the ribbon diagram in Figure (7) are already solved in terms of the linking numbers. Therefore it is only the value of the $3nj = 18j$ (n = 6) symbol which is important. The form (51) also makes reality and symmetry of $\langle \bar{j}_{abcd}|\mathrm{TrU_{abcd}}|j_{abcd}\rangle$ manifest as 3nj symbols of second kind are real

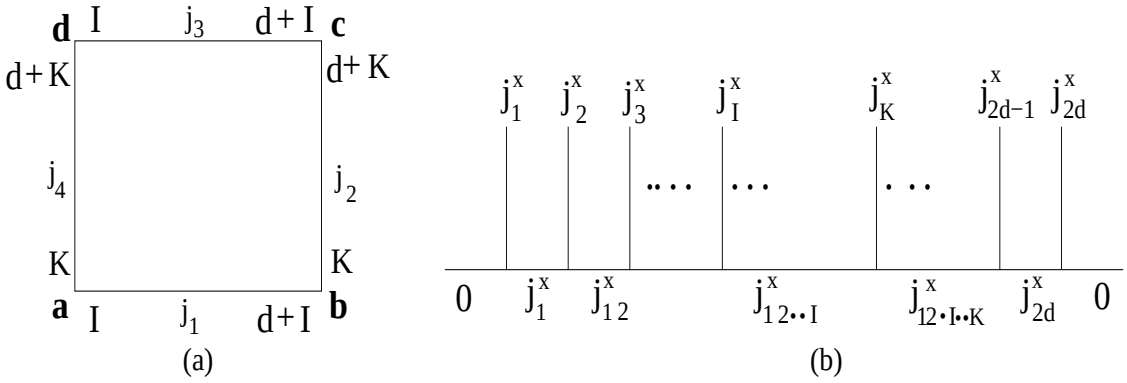

Figure 8: (a) The plaquette **abcd** in the (I, K) plane in d dimension. We choose $I < K,\ 1 \leq I < d$ and $1 < K \leq d$, (b) The angular momentum addition scheme at site x (=**a**,**b**,**c**,**d**). Note that j_1^x and j_{2d}^x appear twice in the scheme. The δ functions are subtracted in (53) to avoid this double counting.

and symmetric:

$$\begin{bmatrix} j_1 & & j_4 & & j_{12}^d & & j_3 & & j_2 & & j_{12}^b & \\ & j_{12}^a & & j_3^d & & j_2^d & & j_{12}^c & & j_1^b & & j_4^b \\ \bar{j}_1 & & \bar{j}_4 & & \bar{j}_{12}^d & & \bar{j}_3 & & \bar{j}_2 & & \bar{j}_{12}^b & \end{bmatrix}$$

$$= \begin{bmatrix} \bar{j}_1 & & \bar{j}_4 & & \bar{j}_{12}^d & & \bar{j}_3 & & \bar{j}_2 & & \bar{j}_{12}^b & \\ & j_{12}^a & & j_3^d & & j_2^d & & j_{12}^c & & j_1^b & & j_4^b \\ j_1 & & j_4 & & j_{12}^d & & j_3 & & j_2 & & j_{12}^b & \end{bmatrix}$$

Before going to arbitrary dimension, we make the following simple observation. Let $\Delta N_x,\ x = a, b, c, d$ denote the number of angular momenta appearing in the loop states $|j_{abcd}\rangle$ in (46) which change under the action of the plaquette operator $\mathrm{Tr}U_{abcd}$ at lattice site x. In the present, $d = 2$, case:

$$\Delta N_a = 2,\ \ (j_1^a, j_2^a)\,;\ \ \Delta N_b = 3,\ \ \left(j_2^b, j_3^b, j_{12}^b\right);\ \ \Delta N_c = 2,\ \ (j_3^c, j_4^c)\,;\ \ \Delta N_d = 3,\ \ \left(j_1^d, j_4^d, j_{12}^d\right).$$

The $U(1)$ identification (47) implies double counting on each of the 4 links of the plaquette *abcd*. Therefore, the number of angular momenta which change under the action of the plaquette in the (12) plane: $\Delta N(12) = \Delta N_a + \Delta N_b + \Delta N_c + \Delta N_d - 4 = 10 - 4 = 6 = n$. This analysis will be useful to generalize the loop dynamics to arbitrary dimensions below.

3.2 d dimension

It is clear from the previous section that the loop dynamics in d dimension is also given in terms of $3nj$ symbols. However, in arbitrary d dimension, n will depend on the orientation of the plaquette. We will now compute n. We consider the plaquette **abcd** in the $(I, K), I < K$ plane as shown in Figure (8). Like in $d = 2$, we consider the loop states over the plaquette *abcd*:

$$|j_{abcd}\rangle \equiv |LS\rangle_a \otimes |LS\rangle_b \otimes |LS\rangle_c \otimes |LS\rangle_d \tag{52}$$

where $|LS\rangle_{x=a,b,c,d} = |j_1^x, j_2^x, j_{12}^x, j_3^x, j_{123}^x, ..., j_I^x, j_{12...I}^x, .., j_K^x, j_{12..I..K}^x, ..., j_{2d-1}^x, j_{12..(2d-1)}^x (= j_{2d}^x), j_{2d}^x, 0\rangle$. We now have to count the the number of angular momenta in (52) which change under the action of

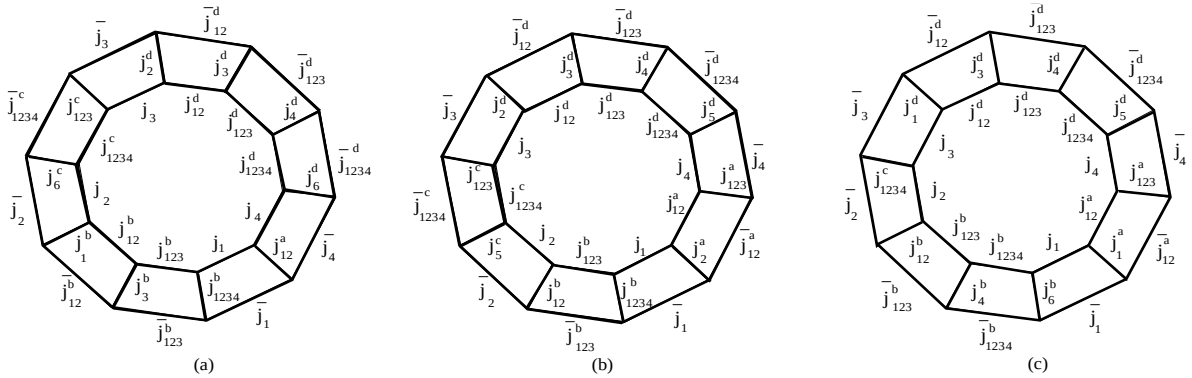

Figure 9: The $30j$ ribbon diagrams representing exact SU(2) loop dynamics without any spurious gauge or loop degrees of freedom in d=3: a) (12) plane, b) (13) plane, c) (23) plane. The angular momenta j_1, j_2, j_3 and j_4 are as shown in Figure (8a). The initial (inner) and final (outer) angular momenta differ by $\frac{1}{2}$.

the plaquette operator $\mathrm{Tr}U_{abcd}$ in the (IK) plane. With the choice $I < K$ $(1 \leq I < d, 1 < K \leq d)$, we have:

$$\begin{aligned} \Delta N_a &= 2 + (K - I) - \delta_{I,1}, \qquad & \Delta N_b &= 2 + (d + I) - K, \\ \Delta N_c &= 2 + (K - I) - \delta_{K,d}, \qquad & \Delta N_d &= 2 + (d + K) - I - \delta_{I,1} - \delta_{K,d} \end{aligned} \tag{53}$$

This implies:

$$\Delta N(IK) = \Delta N_a + \Delta N_b + \Delta N_c + \Delta N_d - 4 = 2\left[2 + d + (K - I) - \delta_{I,1} - \delta_{K,d}\right] = n(IK). \tag{54}$$

Like in d =2 case, we have subtracted 4 in (54) because of U(1) gauge invariance. Note that for d=2, $\Delta N(12) = 6$ and for d=3, $\Delta N(12) = \Delta N(13) = \Delta N(23) = 10$. The d = 3 loop dynamics is explicitly shown in Figure (9) where we have used the notations from Figure (8a), i.e.:

$$\begin{aligned} &(I = 1, K = 2) = (12) \text{ plane} : j_1^a = j_4^b = j_1,\ j_2^b = j_5^c = j_2,\ j_4^c = j_1^d = j_3, j_5^d = j_2^a = j_4, \\ &(I = 1, K = 3) = (13) \text{ plane} : j_1^a = j_4^b = j_1,\ j_3^b = j_6^c = j_2,\ j_4^c = j_1^d = j_3, j_6^d = j_3^a = j_4, \\ &(I = 2, K = 3) = (23) \text{ plane} : j_2^a = j_5^b = j_1,\ j_3^b = j_6^c = j_2,\ j_5^c = j_2^d = j_3, j_6^d = j_3^a = j_4. \end{aligned}$$

It is clear from (54) that in higher $(d > 3)$ dimension $\Delta N(IK)$ depends on the orientation of the plaquette. The corresponding $3n(I, K)j$ symbol describing the loop dynamics in the above angular momentum addition scheme can be easily written down.

4 SU(N) prepotentials

We now briefly discuss the extension of the ideas in this paper to the SU(N) gauge group. The SU(N) generalization of the SU(2) Jordan-Schwinger mapping (11) has been done in [18] in the context of SU(N) coherent states. We define the left and right SU(N) electric fields through the SU(N) prepo-

tentials:

$$E^a_L = \sum_{r=1}^{N-1} E^a_L[r] = \sum_{r=1}^{N-1} a^\dagger[r]\frac{\lambda^a[r]}{2}a[r]; \quad E^a_R = \sum_{r=1}^{N-1} E^a_R[r] = \sum_{r=1}^{N-1} b^\dagger[r]\frac{\lambda^a[r]}{2}b[r]. \tag{55}$$

In (55), the index $r(= 1, 2, ..., (N-1))$ covers all the $(N-1)$ fundamental representations of SU(N) group and all the link indices (n,i) are suppressed. Again, the $(N-1)$ SU(N) Casimirs on the left and the right ends of any link (n,i) are the prepotential number operators:

$$N_a[r] = a^\dagger[r] \cdot a[r], \qquad N_b[r] = b^\dagger[r] \cdot b[r]; \quad r = 1, 2, .., (N-1). \tag{56}$$

The SU(N) kinematical constraints involving SU(N) Casimirs [11] are now in terms of the prepotential number operators:

$$N_a[r](n, i) = N_b[r](n + i, i), \quad r = 1, 2, ..(N-1). \tag{57}$$

The $(N-1)$ constraints (57) are analogous to the single constraint (13) for SU(2). The defining relations (55) for the prepotentials and the constraints (57) imply the following abelian gauge invariance:

$$a^\dagger[r](n, i) \rightarrow expi\theta[r](n, i)\ a^\dagger[r](n, i); \qquad b^\dagger[r](n + i, i) \rightarrow exp - i\theta[r](n, i)\ b^\dagger[r](n + i, i). \tag{58}$$

Thus the SU(N) prepotential formulation will have $SU(N) \otimes (U(1))^{N-1}$ gauge invariance leading to $(N-1)$ varieties of loops. Therefore, using the ideas of SU(N) Schwinger bosons and the corresponding coherent states [18], like in appendix A for SU(2), it should be possible to find an orthonormal loop basis and corresponding loop dynamics for SU(N) lattice gauge theory as well. The work in this direction is in progress.

5 Summary and discussion

In this work we developed ideas and techniques to formulate Hamiltonian lattice gauge theories exactly and most economically in terms of loop and string degrees of freedom. This required systematically solving Gauss law constraints, Mandelstam constraints and finally triangular constraints. The apparently highly non-local and formidable Mandelstam constraints in terms of the link operators were cast and then solved locally in terms of the prepotential intertwining operators. Infact, one of the motivations for this work was to develop manifestly SU(2) gauge invariant techniques involving gauge invariant local intertwining prepotential operators and intertwining/linking quantum numbers having direct geometrical interpretation in terms of loops. The resulting simplifications have been emphasized in the text. Note that the loop states as well as loop dynamics were constructed directly in terms of the above, without using Clebsch-Gordan coefficients which are not gauge invariant and also do not have direct interpretation in terms of loops. The final loop dynamics, i.e., the matrix elements of the magnetic field terms in between the two loop basis states, are found to be real and symmetric and are given by $3nj$ symbol in arbitrary dimension. Therefore, this loop space description of gauge theories is also a non-abelian dual description [12] where the effect of compactness of the gauge group is contained in the integer intertwining or half-integer angular momentum quantum numbers labeling the loop states. In the simpler context of compact (2+1) and (3+1) U(1) gauge theories such duality

transformations are known to isolate the topological magnetic monopole degrees of freedom leading to confinement [27]. It will also be interesting to develop a systematic weak coupling ($g \to 0$) loop perturbation theory near the continuum. This perturbation theory should encapsulate the global gauge invariant loop fluctuations as opposed to the local gauge field fluctuations which is the case with the standard perturbation theory. The issue of color confinement and vacuum structure will be of special interest. The work in this direction is in progress and will be reported elsewhere. The present prepotential approach has also been found useful to study spin networks and analyze the spectrum of the volume operators in lattice loop quantum gravity [28]. Finally, the maximally reduced loop basis and the corresponding matrix elements should also be useful for numerical diagonalization.

This work is dedicated to the memory of late Prof. C. K. Majumdar.

Appendix A

In this section we explicitly construct all possible orthonormal loop states (34) in terms of prepotentials intertwining operators. We appropriately interpret, modify and generalize the techniques developed in [17] to add angular momenta in terms of Schwinger bosons or equivalently prepotentials in our formulation. The basic idea is that angular momenta can be combined directly in terms of prepotentials and the $d(2d-1)$ intertwining operators (19) by taking certain direct products of SU(2) coherent states. We explain this idea in $d = 2$. It's generalization to arbitrary dimension is then obvious and done next. The SU(2) group manifold S^3 is characterized by a doublet of complex numbers (z_1, z_2) with the constraint: $|z_1|^2 + |z_2|^2 = 1$. The SU(2) coherent state in the spin j representation are given by [18]:

$$|z\rangle_j = \sum_{m=-j}^{j} \frac{(z_1)^{j+m}(z_2)^{j-m}}{\sqrt{(j+m)!(j-m)!}} \; |j,m\rangle \equiv \sum_{m=-j}^{j} \phi_{jm}(z) \; |j,m\rangle \tag{59}$$

In terms of Schwinger bosons,

$$|j,m\rangle \equiv \frac{(a_1^\dagger)^{j+m}(a_2^\dagger)^{j-m}}{\sqrt{(j+m)!(j-m)!}} \; |0,0\rangle. \tag{60}$$

The generating function of SU(2) coherent state is:

$$\sum_j \Phi_j(\delta)|z\rangle_j = exp\left(\delta \; z\cdot a^\dagger\right)|0\rangle \equiv exp\left(\delta \; (z_1 a_1^\dagger + z_2 a_2^\dagger)\right)|0\rangle \tag{61}$$

where $\Phi_j(\delta) = \delta^{2j}$. The states $|j,m\rangle$ can be extracted by comparing the terms with coefficients δ^{2j} on both sides of (61). To add the 2 angular momenta, $J^a[1] = a^\dagger[1]\frac{\sigma^a}{2}a[1]$ and $J^a[2] = a^\dagger[2]\frac{\sigma^a}{2}a[2]$, we consider direct product of the generating functions of two SU(2) coherent states defined over the complex planes (x_1, x_2) and (y_1, y_2) respectively.

$$|x\rangle \otimes |y\rangle \equiv \sum_{j_1 j_2} |x\rangle_{j_1} \otimes \; |y\rangle_{j_2} = exp\left(x\cdot a^\dagger[1] + y\cdot a^\dagger[2]\right)|0\rangle \tag{62}$$

We apply the differential operator involving a triplet of complex parameters $(\delta_1, \delta_2, \delta_3)$ and a complex doublet $z(\equiv (z_1, z_2))$:

$$exp\left(\delta_3 \; (\partial_x \cdot \tilde{\partial}_y) + \delta_1 \; (z\cdot\partial_x) + \delta_2 \; (z\cdot\partial_y)\right) \tag{63}$$

on the both sides of (62) and put $x = y = 0$ to get [17]:

$$\sum_{j_1 j_2 j_{12}} \Phi_{j_1 j_2 j_{12}}(\vec{\delta})|z\rangle_{j_{12}}^{j_1 j_2} = exp\Big(\delta_3\ a^\dagger[1]\cdot\tilde{a}^\dagger[2] + z\cdot a^\dagger[12]\Big) = exp\Big(\delta_3\ L_{12} + z\cdot a^\dagger[12]\Big)|0\rangle \tag{64}$$

where L_{12} is the intertwining operator in the (12) plane and

$$a_\alpha^\dagger[12] \equiv \delta_1 a_\alpha^\dagger[1] + \delta_2 a_\alpha^\dagger[2] \tag{65}$$

$$\Phi_{j_1 j_2 j_{12}}(\vec{\delta}) = \left[\frac{(j_1+j_2+j_{12}+1)!}{(2j_{12}+1)}\right]^{\frac{1}{2}} \frac{(\delta_1)^{j_1-j_2+j_{12}}(\delta_2)^{-j_1+j_2+j_{12}}(\delta_3)^{j_1+j_2-j_{12}}}{[(j_1-j_2+j_{12})!(-j_1+j_2+j_{12})!(j_1+j_2-j_{12})!]^{\frac{1}{2}}} \tag{66}$$

In (64), $|z\rangle_{j_{12}}^{j_1 j_2}$ is the coherent state in the j_{12} representation of the combined angular momentum $(\vec{J}[1]+\vec{J}[2])$, i.e:

$$|z\rangle_{j_{12}}^{j_1 j_2} \equiv \sum_{m_{12}=-j_{12}}^{+j_{12}} \phi_{j_{12}m_{12}}(z)|j_1 j_2 j_{12} m_{12}\rangle \tag{67}$$

Note that $(j_1 - j_2 + j_{12}), (-j_1 + j_2 + j_{12})$ and $(j_1 + j_2 - j_{12})$ are all non-negative integers due to angular momentum addition rules. The coherent state generating function (64) in the representation j_{12} ($|j_1 - j_2| \le j_{12} \le j_1 + j_2$) is the generalization of the generating function (61) in the case of single angular momentum. To illustrate this, we put $\delta_2 = \delta_3 = 0 (\Rightarrow j_2 = 0, j_1 = j_{12})$ in (64) to recover (61). Now to project out $J_{total} = J[1] + J[2] = 0$ ("gauge invariant state in d = 1") state from the left hand side of (64), we put:

$$\delta_1 = 0, \quad \delta_2 = 0 \quad \Rightarrow \quad j_1 = j_2 \equiv j, \quad j_{total} = j_{12} = 0.$$

Now (64) takes the form:

$$|j_1 = j, j_2 = j, j_{total} = j_{12} = 0\rangle = \mathcal{N}(j)\frac{(L_{12})^{l_{12}}}{(l_{12})!}\ |0\rangle \tag{68}$$

In (68) $l_{12} = 2j$ and

$$\mathcal{N}(j) = N(j_1 = j, j_2 = j, j_{12} = 0) = \frac{1}{\sqrt{(2j+1)}} \tag{69}$$

In (69), $N(j_1, j_2, j_{12}) = \sqrt{\frac{(2j_{12}+1)}{(j_1+j_2+j_{12}+1)!}}\,[(-j_1+j_2+j_{12})!(j_1-j_2+j_{12})!(j_1+j_2-j_{12})!]^{\frac{1}{2}}$ are the normalization constant so that $\langle j_1 = j, j_2 = j, j_{total} = j_{12} = 0|j_1 = j, j_2 = j, j_{total} = j_{12} = 0\rangle = 1$. The U(1) Gauss law makes j site independent. These states are the trivial examples of the "loop states" in d=1. We now generalize the above simple construction in d=1 to d=2. To add the third angular momentum corresponding to $a^\dagger[n,3]$ we rewrite (64) with $z \to x$ and take the direct product with

$$|y\rangle \equiv \sum_{j_3 m_3} \phi_{j_3 m_3}(y)|j_3, m_3\rangle = exp(y.a^\dagger[3])|0\rangle$$

We now apply the operator (63) with $\delta \to \sigma$:

$$exp\Big(\sigma_3\ (\partial_x\cdot\tilde{\partial}_y) + \sigma_1\ (z\cdot\partial_x) + \sigma_2\ (z\cdot\partial_y)\Big) \tag{70}$$

to get:

$$\sum_{j_1 j_2 j_{12} j_3 j_{123}} \Phi_{j_1 j_2 j_{12}}(\vec{\delta})\Phi_{j_{12} j_3 j_{123}}(\vec{\sigma})|z\rangle_{j_{123}}^{j_1 j_2 j_{12} j_3} = exp\left(L_{123} + z.a^\dagger[123]\right)\ |0\rangle \tag{71}$$

where,

$$\begin{aligned} a^\dagger[123] &\equiv \sigma_1 a^\dagger[12] + \sigma_2 a^\dagger[3] \\ L_{123} \equiv \delta_3\ a^\dagger[1].\tilde{a}^\dagger[2] + \sigma_3\ a^\dagger[12].\tilde{a}^\dagger[3] &= \delta_3 L_{12} + \sigma_3\left(\delta_1 L_{13} + \delta_2 L_{23}\right). \end{aligned} \tag{72}$$

and

$$|z\rangle_{j_{12} j_{123}}^{j_1 j_2 j_3} \equiv \sum_{m_{123}=-j_{123}}^{+j_{123}} \phi_{j_{123} m_{123}}(z)|j_1 j_2 j_{12} j_3 j_{123} m_{123}\rangle$$

is the SU(2) coherent states in the combined angular momentum $\vec{J}[123] = \left(\left(\vec{J}[1] + \vec{J}[2]\right) + \vec{J}[3]\right)$ representation with $|j_{12} - j_3| \leq j_{123} \leq j_{12} + j_3$. The operator L_{123} contains the intertwining operators in the (12), (13) and (23) planes. Note that, like in the previous case, putting $\sigma_2 = \sigma_3 = 0 (\Rightarrow j_3 = 0, j_{123} = j_{12})$ in (72) we recover (64). Therefore, it is a sequential process. Repeating the same steps once again in the 4^{th} direction with the prepotential operators $a^\dagger[4]$, we finally get:

$$\sum_{j_1 j_2 j_{12} j_3 j_{123} j_{1234}} \Phi_{j_1 j_2 j_{12}}(\vec{\delta})\Phi_{j_{12} j_3 j_{123}}(\vec{\sigma})\Phi_{j_{123} j_4 j_{1234}}(\vec{\rho})|z\rangle_{j_{1234}}^{j_1 j_2 j_{12} j_3 j_{123} j_4} = exp\ \left(L_{1234} + z.a^\dagger[1234]\right)\ |0\rangle \tag{73}$$

where, $a^\dagger[1234] \equiv \rho_1 a^\dagger[123] + \rho_2 a^\dagger[4]$ and L_{1234} contains intertwining in (12), (13), (14), (23), (24) and (34) planes:

$$\begin{aligned} L_{1234} &\equiv \delta_3\ a^\dagger[1]\cdot\tilde{a}^\dagger[2] + \sigma_3\ a^\dagger[12]\cdot\tilde{a}^\dagger[3] + \rho_3 a^\dagger[123]\cdot\tilde{a}^\dagger[4] \\ &= \delta_3\left(L_{12}\right) + \sigma_3\left(\delta_1 L_{13} + \delta_2 L_{23}\right) + \rho_3\left(\sigma_1\delta_1 L_{14} + \sigma_1\delta_2 L_{24} + \sigma_2 L_{34}\right) \end{aligned} \tag{74}$$

The gauge invariant states can now be projected (like in d=1 case) by choosing:

$$\vec{\rho} = (0, 0, \rho_3) \quad => \quad j_{123} = j_4, \quad j_{1234} = 0.$$

We now compare the coefficients of $(\delta_1, \delta_2, \delta_3)$, $(\sigma_1, \sigma_2, \sigma_3)$ and ρ_3 to get the all possible manifestly gauge invariant orthonormal states at site n. After some algebra we get[10]:

$$\begin{aligned} |j_1, j_2, j_{12}\rangle &\equiv |j_1, j_2, j_{12}, (j_3), j_{123} = (j_4), j_4, j_{total} = j_{1234} = 0, m_{total} = m_{1234} = 0\rangle \\ &= \mathcal{N}(j) \sum_{\substack{l_{13}, l_{14} \\ l_{23}, l_{24}}}{}' \prod_{\substack{i,j \\ i<j}} \frac{\left(L_{ij}(n)\right)^{l_{ij}}}{(l_{ij})!}|0\rangle \end{aligned} \tag{75}$$

In (75), $\mathcal{N}(j)$ is the constant given in terms of $N(j_1, j_2, j_{12})$ in (66):

$$\mathcal{N}(j) = N(j_1, j_2, j_{12})\ N(j_{12}, j_3, j_4)\ N(j_4, j_4, 0) \tag{76}$$

so that the states in (75) are normalized to unity. The d=2 results (75) and (76) are analogous to d=1 results given in (68) and (69) respectively. The difference is the summation over the linking

[10]Note that we have solved the SU(2) Gauss law at a site n and have ignored the site index from j^s and l^s.

numbers in (75) which was missing in (68). This is because now there are many possibilities of linking or contracting the 4 types of Young boxes representing $a^\dagger[1], a^\dagger[2], a^\dagger[3]$ and $a^\dagger[4]$ mutually to produce $j_{total} = 0$ states. These contractions must be such that the states (75) are the eigenstates of the CSCO(I) as well as CSCO(II) listed in (28). In the construction (75) the linking numbers have to satisfy:

$$\sum_{j=1}^{2d} l_{ij} = 2j_i, \quad i = 1, 2, .., 2d. \tag{77}$$

and

$$\begin{aligned} l_{12} &= j_1 + j_2 - j_{12} \\ l_{13} + l_{23} &= j_{12} + j_3 - j_{123} = j_{12} + j_3 - j_4 \\ l_{14} + l_{24} + l_{34} &= j_{123} + j_4 - j_{1234} = 2j_4. \end{aligned} \tag{78}$$

ensuring that the states are common eigenstates of CSCO(I) and CSCO(II) respectively. The constraints (77) and (78) on the linking numbers are denoted by the $\prime$ over the summation sign in (75). The last constraint in (78) represents the partition of j_4 in terms of the linking numbers and is already contained in (77). Note that we have combined angular momenta directly in terms of l_{ij} without using any Clebsch-Gordon coefficients containing magnetic quantum numbers. The generalization of these techniques to arbitrary dimension is a sequential process and the results are given in (34).

Appendix B

In this appendix, we compute the SU(2) loop dynamics. As mentioned before the electric field term in (43) simply counts the abelian flux lines without changing the loop states. The action of the magnetic field term in (43) on the loop states is non-trivial. The calculations of the matrix elements of $\mathrm{Tr}U_\square$ in d=2 are presented below. It is convenient to define the square root of the multiplicity factors:

$$\Pi(x, y, ...) \equiv \sqrt{(2x+1)(2y+1)....},$$

which will occur repeatedly below.

The matrix elements of an intertwining operators $L_{12} = \left(a^\dagger[1] \cdot \tilde{a}^\dagger[2]\right)$ in the corresponding angular momentum basis $|j_1, j_2, j_{12}, m_{12}\rangle$ are given by the generalized Wigner Eckart theorem [25, 26]:

$$\begin{aligned} &\langle \bar{j}_1, \bar{j}_2, \bar{j}_{12}, \bar{m}_{12}| \left(a^\dagger[1] \cdot \tilde{a}^\dagger[2]\right) |j_1, j_2, j_{12}, m_{12}\rangle = \sqrt{2}\ \langle \bar{j}_1, \bar{j}_2, \bar{j}_{12}, \bar{m}_{12}| \left(a^\dagger[1] \otimes a^\dagger[2]\right)^0_0 |j_1, j_2, j_{12}, m_{12}\rangle \\ &= \sqrt{2}\ (-1)^{(\bar{j}_{12} - \bar{m}_{12})}\ \Pi(j_{12}, \bar{j}_{12}, 0) \begin{pmatrix} \bar{j}_{12} & 0 & j_{12} \\ -\bar{m}_{12} & 0 & m_{12} \end{pmatrix} \begin{Bmatrix} \bar{j}_1 & j_1 & \frac{1}{2} \\ \bar{j}_2 & j_2 & \frac{1}{2} \\ \bar{j}_{12} & j_{12} & 0 \end{Bmatrix} \langle \bar{j}_1 || a^\dagger[1] || j_1 \rangle \langle \bar{j}_2 || a^\dagger[2] || j_2 \rangle \end{aligned}$$

In (79), $\left(a^\dagger[1] \otimes a^\dagger[2]\right)^0_0 \equiv \sum_{m,\bar{m}=\pm\frac{1}{2}} C^{0,0}_{\frac{1}{2},m;\frac{1}{2},\bar{m}} a^\dagger_m b^\dagger_{\bar{m}}$ with $a_{+\frac{1}{2}} \equiv a_1,\ a_{-\frac{1}{2}} \equiv a_2$. The reduced matrix elements of the prepotential operators are given by:

$$\langle \bar{j} || a || j \rangle = \Pi(j, \bar{j})\ \delta_{\bar{j}, j-\frac{1}{2}}, \qquad \langle \bar{j} || a^\dagger || j \rangle = \Pi(j, \bar{j})\ \delta_{\bar{j}, j+\frac{1}{2}}. \tag{79}$$

The coefficients $\begin{pmatrix} j_1 & j_2 & j_3 \\ m_1 & m_2 & m_3 \end{pmatrix}, \begin{Bmatrix} j_1 & j_2 & j_{12} \\ j_3 & j_4 & j_{34} \\ j_{13} & j_{24} & j \end{Bmatrix}$ represent $3j$ and $9j$ symbols [25] respectively.

Using the values:

$$\begin{pmatrix} \bar{j}_{12} & 0 & j_{12} \\ -\bar{m}_{12} & 0 & m_{12} \end{pmatrix} = \frac{(-1)^{-\bar{j}_{12}+\bar{m}_{12}}}{\Pi(j_{12})} \delta_{j_{12},\bar{j}_{12}}\delta_{m_{12},\bar{m}_{12}},$$

$$\begin{Bmatrix} \bar{j}_1 & j_1 & \frac{1}{2} \\ \bar{j}_2 & j_2 & \frac{1}{2} \\ \bar{j}_{12} & j_{12} & 0 \end{Bmatrix} = \frac{(-1)^{j_1+\frac{1}{2}+\bar{j}_2+\bar{j}_{12}}}{\Pi(\frac{1}{2},j_{12})} \delta_{j_{12},\bar{j}_{12}} \begin{Bmatrix} \bar{j}_1 & j_1 & \frac{1}{2} \\ j_2 & \bar{j}_2 & j_{12} \end{Bmatrix},$$

we get:

$$\langle \bar{j}_1, \bar{j}_2, \bar{j}_{12}, \bar{m}_{12}|L_{12}|j_1, j_2, j_{12}, m_{12}\rangle = \delta_{j_{12},\bar{j}_{12}}\delta_{m_{12},\bar{m}_{12}}(-1)^{j_{12}}\eta(j_1,\bar{j}_2) \begin{Bmatrix} \bar{j}_1 & j_1 & \frac{1}{2} \\ j_2 & \bar{j}_2 & j_{12} \end{Bmatrix}$$
$$\langle \bar{j}_1||a^\dagger[1]||j_1\rangle\langle \bar{j}_2||a^\dagger[2]||j_2\rangle. \quad (80)$$

In (80), the phase factor $\eta(a,b) \equiv (-1)^{a+b+\frac{1}{2}}$. Note that one can also apply the above intertwining operator directly on the loop basis (75) to get it's matrix elements (80) algebraically. Infact, this has provided an independent check on the "master formula" (80) which is crucial for the computations below. It simply states that the intertwining operator $L_{12} = a^\dagger[1] \cdot \tilde{a}^\dagger[2]$ increases j_1 and j_2 by $\frac{1}{2}$. Further, as L_{12} commutes with the $(J[1] + J[2])^2$, the matrix elements are diagonal in j_{12} and m_{12}. The matrix elements of the intertwining operators in the geometrical form (80) also tell us that all the 16 terms in $\sum_{\alpha\beta\gamma\delta=\pm} H_{\alpha\beta\gamma\delta}$ in (45) differ only in their reduced matrix element structures. Therefore, we need to compute the matrix elements of only a single term in (45), providing enormous simplification at the algebraic level. In the following calculations, we choose this term to be the first term in (45) associated with the plaquette *abcd* in Figure (5):

$$H_{++++} \equiv F_{abcd} \left(a^\dagger[1] \cdot \tilde{a}^\dagger[2]\right)_a \left(a^\dagger[2] \cdot \tilde{a}^\dagger[3]\right)_b \left(a^\dagger[3] \cdot \tilde{a}^\dagger[4]\right)_c \left(a^\dagger[4] \cdot \tilde{a}^\dagger[1]\right)_d F_{abcd} \quad (81)$$

As mentioned in the beginning of this section, we will work in $d = 2$. The results are then easily generalized to arbitrary dimensions d and are given in the equation (51). In computing the loop dynamics below, it will be often convenient to change the angular momentum addition scheme[11]:

$$|j_1, j_2, j_3, j_4, j_{12}\rangle \equiv |j_1, j_2, j_{12}, j_3, j_{123}(= j_4), j_4, j_{total} = j_{(123)(4)} = 0\rangle$$
$$= |(j_1, j_2)j_{12}, (j_3, j_4)j_{34}(= j_{12}), j_{total} = j_{(12)(34)} = 0\rangle \equiv |(j_1, j_2)j_{12}, (j_3, j_4)j_{12}\rangle \quad (82)$$

[11]The relation (82) is proved by writing:

$$|j_1, j_2, j_3, j_4, j_{12}\rangle \equiv \sum_{all\ m} C^{0,0}_{j_{123}m_{123},j_4m_4} C^{j_{123},m_{123}}_{j_{12}m_{12},j_3m_3} |j_1, j_2, j_{12}, m_{12}\rangle|j_3m_3\rangle|j_4m_4\rangle$$
$$= \sum_{all\ m} \sum_{j_{34}} C^{0,0}_{j_{12}m_{12},j_{34}m_{34}} |j_1, j_2, j_{12}, m_{12}\rangle|j_3, j_4, j_{34}, m_{34}\rangle = |(j_1, j_2)j_{12}, (j_3, j_4)j_{12}\rangle.$$

We have used:

$$C^{0,0}_{j^a_{123}m^a_{123},j^a_4m^a_4} = \frac{(-1)^{j^a_4+m^a_4}}{\Pi(j^a_4)}\delta_{j^a_{123},j^a_4}\delta_{m^a_{123},-m^a_4}, \quad \frac{(-1)^{j^a_4+m^a_4}}{\Pi(j^a_4)} C^{j^a_4-m^a_4}_{j^a_{12}m^a_{12},j^a_3m^a_3} = C^{0,0}_{j^a_{12}m^a_{12},j^a_{12}-m^a_{12}} C^{j^a_{12}-m^a_{12}}_{j^a_3m^a_3,j^a_4m^a_4}.$$

The equivalent scheme on the right of (82) simplifies the algebra. We also note that the normalization operator F_{abcd} in (45) has simple action on the loop states $|j_{abcd}\rangle$ defined in (46)and (47):

$$F_{abcd}|j_{abcd}\rangle = \frac{1}{\Pi(j_1, j_2, j_3, j_4)}|j_{abcd}\rangle \tag{83}$$

Therefore, we only need to compute the matrix elements of the intertwining operators in (81) in the orthonormal loop basis given in (75).

Loop dynamics at a:

In H_{++++} above, the intertwining operator at a is $\left(a^\dagger[1]\cdot\tilde{a}^\dagger[2]\right)_a$. Using (80), one directly gets:

$$\langle \bar{j}_1^a, \bar{j}_2^a, \bar{j}_3^a, \bar{j}_4^a, \bar{j}_{12}^a|\left(a^\dagger[1]\cdot\tilde{a}^\dagger[2]\right)_a|j_1^a, j_2^a, j_3^a, j_4^a, j_{12}^a\rangle = (-1)^{j_{12}^a}\eta(j_1^a, \bar{j}_2^a)\delta_{j_3^a,\bar{j}_3^a}\delta_{j_4^a,\bar{j}_4^a}\delta_{j_{12}^a,\bar{j}_{12}^a}$$
$$\left\{\begin{array}{ccc} j_1^a & \bar{j}_1^a & \frac{1}{2} \\ \bar{j}_2^a & j_2^a & j_{12}^a \end{array}\right\}\langle \bar{j}_1^a||a^\dagger[1]||j_1^a\rangle\langle \bar{j}_2^a||a^\dagger[2]||j_2^a\rangle \tag{84}$$

The intertwining operator $\left(a^\dagger[1]\cdot\tilde{a}^\dagger[2]\right)_a$ increases the SU(2) flux on the links l_1 as well as l_4 of Figure (5). Note that this information is contained only in the last two reduced matrix element terms in (84).

Loop dynamics at b:

The intertwining operator at b in (81) is $\left(a^\dagger[2]\cdot\tilde{a}^\dagger[3]\right)_b$. To compute it's action at b, we write the loop states (34) in terms of the basis states which diagonalize $(J[2]+J[3])^2$:

$$\begin{aligned} |j_1^b j_2^b j_3^b j_4^b j_{12}^b\rangle &= (-1)^{(j_1^b+j_2^b+j_3^b+j_{123}^b)}\sum_{j_{23}^b}\Pi(j_{12}^b, j_{23}^b)\left\{\begin{array}{ccc} j_1^b & j_2^b & j_{12}^b \\ j_3^b & j_{123}^b & j_{23}^b \end{array}\right\}|j_1^b j_2^b j_3^b j_4^b j_{23}^b\rangle \\ &= (-1)^{(j_1^b+j_2^b+j_3^b+j_4^b)}\sum_{j_{23}^b}\Pi(j_{12}^b, j_{23}^b)\left\{\begin{array}{ccc} j_1^b & j_2^b & j_{12}^b \\ j_3^b & j_4^b & j_{23}^b \end{array}\right\}|j_1^b j_2^b j_3^b j_4^b j_{23}^b\rangle \end{aligned} \tag{85}$$

In (85), $|j_1^b j_2^b j_3^b j_4^b j_{23}^b\rangle \equiv |j_1^b, (j_2^b j_3^b), j_{23}^b, j_{123}^b, j_4^b, j_{1234}^b = m_{1234}^b = 0\rangle$ and we have used $j_{123} = j_4$. Note that the phase factor $(-1)^{(j_1^b+j_2^b+j_3^b+j_4^b)}$ in (85) is real because of the triangular constraints on the angular momenta or equivalently (24). Now we use:

$$|j_1^b j_2^b j_3^b j_4^b j_{23}^b\rangle = (-1)^{2j_1^b}|j_2^b j_3^b j_4^b j_1^b j_{23}^b = j_{41}^b\rangle \tag{86}$$

and (80) to get:

$$\langle \bar{j}_1^b, \bar{j}_2^b, \bar{j}_3^b, \bar{j}_4^b, \bar{j}_{12}^b|\left(a^\dagger[2]\cdot\tilde{a}^\dagger[3]\right)_b|j_1^b, j_2^b, j_3^b, j_4^b, j_{12}^b\rangle = (-1)^{j_2^b+j_3^b-\bar{j}_2^b-\bar{j}_3^b}\eta(j_2^b, \bar{j}_3^b)\delta_{j_1^b,\bar{j}_1^b}\delta_{j_4^b,\bar{j}_4^b}\Pi(j_{12}^b, \bar{j}_{12}^b)$$

$$\sum_{j_{23}^b}(-)^{j_{23}^b}\Pi(j_{23}^b)\left\{\begin{array}{ccc} j_3^b & j_2^b & j_{23}^b \\ j_1^b & j_4^b & j_{12}^b \end{array}\right\}\left\{\begin{array}{ccc} j_1^b & \bar{j}_4^b & j_{23}^b \\ \bar{j}_3^b & j_2^b & \bar{j}_{12}^b \end{array}\right\}\left\{\begin{array}{ccc} \bar{j}_3^b & \bar{j}_2^b & j_{23}^b \\ j_2^b & j_3^b & \frac{1}{2} \end{array}\right\}\langle \bar{j}_2^b||a^\dagger[2]||j_2^b\rangle\langle \bar{j}_3^b||a^\dagger[3]||j_3^b\rangle$$

The summation over j_{23}^b in the last line above can be performed using Biedenharn-Elliot identity [25]:

$$\sum_x(-1)^x\Pi^2(x)\left\{\begin{array}{ccc} a & b & x \\ c & d & p \end{array}\right\}\left\{\begin{array}{ccc} c & d & x \\ e & f & q \end{array}\right\}\left\{\begin{array}{ccc} e & f & x \\ b & a & s \end{array}\right\} = (-1)^{-r}\left\{\begin{array}{ccc} p & q & s \\ e & a & d \end{array}\right\}\left\{\begin{array}{ccc} p & q & s \\ f & b & c \end{array}\right\}$$
$$r = (a+b+c+d+e+f+p+q+s).$$

Finally, the loop dynamics at lattice site b is given by:

$$\langle \bar{j}_1^b, \bar{j}_2^b, \bar{j}_3^b, \bar{j}_4^b, \bar{j}_{12}^b| \left(a^\dagger[2]\cdot\tilde{a}^\dagger[3]\right)_b |j_1^b, j_2^b, j_3^b, j_4^b, j_{12}^b\rangle = (-1)^{j_1^b+j_4^b}\eta(j_2^b,\bar{j}_3^b)\eta(j_{12}^b,\bar{j}_{12}^b)\delta_{j_1^b,\bar{j}_1^b}\delta_{j_4^b,\bar{j}_4^b}$$

$$\Pi(j_{12}^b,\bar{j}_{12}^b)\left\{\begin{array}{ccc} j_{12}^b & \bar{j}_{12}^b & \frac{1}{2} \\ \bar{j}_3^b & j_3^b & j_4^b \end{array}\right\}\left\{\begin{array}{ccc} j_{12}^b & \bar{j}_{12}^b & \frac{1}{2} \\ \bar{j}_2^b & j_2^b & j_1^b \end{array}\right\}\langle\bar{j}_2^b||a^\dagger[2]||j_2^b\rangle\langle\bar{j}_3^b||a^\dagger[3]||j_3^b\rangle \qquad (87)$$

Loop dynamics at c:

At c, we use (82) to write

$$|j_1^c, j_2^c, j_3^c, j_4^c, j_{12}^c\rangle = |(j_1^c, j_2^c)j_{12}^c, (j_3^c j_4^c), j_{12}^c\rangle = (-1)^{2j_{12}^c}|(j_3^c, j_4^c)j_{12}^c, (j_1^c j_2^c)j_{12}^c\rangle$$

to get:

$$\langle \bar{j}_1^c, \bar{j}_2^c, \bar{j}_3^c, \bar{j}_4^c, \bar{j}_{12}^c| \left(a^\dagger[3]\cdot\tilde{a}^\dagger[4]\right)_c |j_1^c, j_2^c, j_3^c, j_4^c, j_{12}^c\rangle = (-1)^{j_{12}^c}\eta(j_3^c,\bar{j}_4^c)\delta_{j_1^c,\bar{j}_1^c}\delta_{j_2^c,\bar{j}_2^c}\delta_{j_{12}^c,\bar{j}_{12}^c}$$
$$\left\{\begin{array}{ccc} j_3^c & \bar{j}_3^c & \frac{1}{2} \\ \bar{j}_4^c & j_4^c & j_{12}^c \end{array}\right\}\langle\bar{j}_3^c||a^\dagger[3]||j_3^c\rangle\langle\bar{j}_4^c||a^\dagger[4]||j_4^c\rangle \qquad (88)$$

Loop dynamics at d:

To compute the loop dynamics at d, we write:

$$|j_1^d, j_2^d, j_3^d, j_4^d, j_{12}^d\rangle = |j_1^d, j_2^d, j_{12}^d, j_3^d, j_4^d, j_{34}^d(=j_{12}^d)\rangle$$

$$\begin{aligned} &= \sum_{j_{14}^d}(-1)^{j_3^d+j_4^d-j_{12}^d}\Pi(j_{12}^d, j_{34}^d, j_{14}^d, j_{23}^d)\left\{\begin{array}{ccc} j_1^d & j_2^d & j_{12}^d \\ j_4^d & j_3^d & j_{34}^d=j_{12}^d \\ j_{14}^d & j_{23}^d=j_{14}^d & 0 \end{array}\right\}|j_4^d, j_1^d, j_{14}^d, j_2^d, j_3^d, j_{23}^d\rangle \\ &= (-1)^{2j_4^d}\sum_{j_{14}}\Pi(j_{12}^d, j_{14}^d)(-1)^{j_1^d+j_2^d+j_3^d+j_4^d}\left\{\begin{array}{ccc} j_1^d & j_2^d & j_{12}^d \\ j_3^d & j_3^d & j_{14}^d \end{array}\right\}|j_4^d, j_1^d, j_{14}^d, j_2^d, j_3^d, j_{23}^d\rangle \qquad (89) \end{aligned}$$

In (89), we have used $\left\{\begin{array}{ccc} j_1^d & j_2^d & j_{12}^d \\ j_4^d & j_3^d & j_{12}^d \\ j_{14}^d & j_{14}^d & 0 \end{array}\right\} = (-1)^{j_2^d+j_{12}^d+j_4^d+j_{14}^d}\left(\Pi(j_{12}^d, j_{14}^d)\right)^{-1}\left\{\begin{array}{ccc} j_1^d & j_2^d & j_{12}^d \\ j_3^d & j_3^d & j_{14}^d \end{array}\right\}.$

Finally, using (89) and the Biedenharn-Elliot identity, the dynamics at d is given by:

$$\langle \bar{j}_1^d, \bar{j}_2^d, \bar{j}_3^d, \bar{j}_4^d, \bar{j}_{12}^d| \left(a^\dagger[4]\cdot\tilde{a}^\dagger[1]\right)_d |j_1^d, j_2^d, j_3^d, j_4^d, j_{12}^d\rangle = -(-1)^{j_2^d+j_3^d}\eta(j_4^d,\bar{j}_1^d)\eta(j_{12}^d,\bar{j}_{12}^d)\delta_{j_2^d,\bar{j}_2^d}\delta_{j_3^d,\bar{j}_3^d}$$

$$\Pi(j_{12}^d,\bar{j}_{12}^d)\left\{\begin{array}{ccc} j_{12}^d & \bar{j}_{12}^d & \frac{1}{2} \\ \bar{j}_1^d & j_1^d & j_2^d \end{array}\right\}\left\{\begin{array}{ccc} j_{12}^d & \bar{j}_{12}^d & \frac{1}{2} \\ \bar{j}_4^d & j_4^d & j_3^d \end{array}\right\}\langle\bar{j}_4^d||a^\dagger[4]||j_4^d\rangle\langle\bar{j}_1^d||a^\dagger[1]||j_1^d\rangle \qquad (90)$$

Loop dynamics at abcd:

We now weave or glue the dynamics at a,b,c,d with the help of U(1) Gauss law (47): $j_1^a = j_3^b \equiv j_1,\ j_2^b = j_4^c \equiv j_2,\ j_3^c = j_1^d \equiv j_3,\ j_4^d = j_2^a \equiv j_4$ and $\bar{j}_1^a = \bar{j}_3^b \equiv \bar{j}_1,\ \bar{j}_2^b = \bar{j}_4^c \equiv \bar{j}_2,\ \bar{j}_3^c = \bar{j}_1^d \equiv \bar{j}_3,\ \bar{j}_4^d = \bar{j}_2^a \equiv \bar{j}_4$. This

implies:

$$\langle \bar{j}_1^a||a^\dagger[1]||j_1^a\rangle = \langle \bar{j}_3^b||a^\dagger[3]||j_3^b\rangle = \Pi(j_1,\bar{j}_1)\delta_{\bar{j}_1,j_1+\frac{1}{2}},\ \langle \bar{j}_2^b||a^\dagger[2]||j_2^b\rangle = \langle \bar{j}_4^c||a^\dagger[4]||j_4^c\rangle = \Pi(j_2,\bar{j}_2)\delta_{\bar{j}_2,j_2+\frac{1}{2}}$$
$$\langle \bar{j}_3^c||a^\dagger[3]||j_3^c\rangle = \langle \bar{j}_1^d||a^\dagger[1]||j_1^d\rangle = \Pi(j_3,\bar{j}_3)\delta_{\bar{j}_3,j_3+\frac{1}{2}},\ \langle \bar{j}_4^d||a^\dagger[4]||j_4^d\rangle = \langle \bar{j}_2^a||a^\dagger[2]||j_2^a\rangle = \Pi(j_4,\bar{j}_4)\delta_{\bar{j}_4,j_4+\frac{1}{2}}$$

Using the U(1) identifications and (83), (84), (87), (88) and (90) and merging all these equations carefully, we get:

$$\langle \bar{j}_{abcd}|\mathrm{T}rU_{abcd}|j_{abcd}\rangle = -\delta_{j_3^a,\bar{j}_3^a}\delta_{j_4^a,\bar{j}_4^a}\delta_{j_{12}^a,\bar{j}_{12}^a}\delta_{j_1^b,\bar{j}_1^b}\delta_{j_4^b,\bar{j}_4^b}\delta_{j_1^c,\bar{j}_1^c}\delta_{j_2^c,\bar{j}_2^c}\delta_{j_{12}^c,\bar{j}_{12}^c}\delta_{j_2^d,\bar{j}_2^d}\delta_{j_3^d,\bar{j}_3^d}(-1)^{j_{12}^a+j_{12}^c}$$

$$(-1)^{j_1^b+j_4^b+j_2^d+j_3^d}\bar{\Pi}(j_1\bar{j}_1)\bar{\Pi}(j_2\bar{j}_2)\bar{\Pi}(j_3\bar{j}_3)\bar{\Pi}(j_4\bar{j}_4)\bar{\Pi}(j_{12}^b\bar{j}_{12}^b)\bar{\Pi}(j_{12}^d\bar{j}_{12}^d)\left\{\begin{array}{ccc} j_1 & \bar{j}_1 & \frac{1}{2} \\ \bar{j}_4 & j_4 & j_{12}^a \end{array}\right\}\left\{\begin{array}{ccc} j_{12}^b & \bar{j}_{12}^b & \frac{1}{2} \\ \bar{j}_1 & j_1 & j_4^b \end{array}\right\}$$

$$\left\{\begin{array}{ccc} j_{12}^b & \bar{j}_{12}^b & \frac{1}{2} \\ \bar{j}_2 & j_2 & j_1^b \end{array}\right\}\left\{\begin{array}{ccc} j_3 & \bar{j}_3 & \frac{1}{2} \\ \bar{j}_2 & j_2 & j_{12}^c \end{array}\right\}\left\{\begin{array}{ccc} j_{12}^d & \bar{j}_{12}^d & \frac{1}{2} \\ \bar{j}_3 & j_3 & j_2^d \end{array}\right\}\left\{\begin{array}{ccc} j_{12}^d & \bar{j}_{12}^d & \frac{1}{2} \\ \bar{j}_4 & j_4 & j_3^d \end{array}\right\} \tag{91}$$

In (91), $\bar{\Pi}(a,b) \equiv (-1)^{a+b+\frac{1}{2}}\Pi(a,b)$. Note that $\bar{\Pi}(a,b)$ are symmetric $\bar{\Pi}(a,b) = \bar{\Pi}(b,a)$ and real. We have ignored the 16 δ functions $\prod_{i=1}^4\left(\delta_{\bar{j}_i,j_i+\frac{1}{2}} + \delta_{\bar{j}_i,j_i-\frac{1}{2}}\right)$ coming from the reduced matrix elements in (79) as they are already contained in the six $6j$ symbols in (91). The above d=2 loop dynamics and it's generalization to arbitrary dimensions are discussed in detail in sections (3.1) and (3.2).

References

[1] S. Mandelstam, Ann. Phys. (N.Y.) **19** (1962) 1; S. Mandelstam, Phys. Rev. **175** (1968) 1580; S. Mandelstam, Phys. Rev. **D 19** (1979) 2391.

[2] K. G. Wilson, Phys. Rev. **D 10** (1974) 2445.

[3] T. T. Wu, C. N. Yang, Phys. Rev. **D 12** (1975) 3845.

[4] A. M. Polyakov, Phys. Lett. **B 82** (1979) 247; A. A. Migdal, Phys. Rep. **102** (1983) 199; A. M. Polyakov, Nucl. Phys. **B164** (1979) 171; N. Nambu, Phys. Lett. **B 80** (1979) 372; J. L. Gervais, A. Neveu, Phys. Lett. **B 80** (1979) 255; Yu. M. Makeenko and A. A. Migdal, Phys. Lett. **B88** (1979) 135; Y. M. Makeenko, A. A. Migdal, Nucl. Phys. **B 188** (1981) 269; F. Gliozzi, T. Reggeand M. A. Virasoro, Phys. Lett. **B81** (1979) 178; M. Virasoro, Phys. Lett. **B 82** (1979) 436; A. Jevicki and B. Sakita, Phys. Rev. **D 22** (1974) 467; A. M. Polyakov, Gauge Fields and Strings (Harwood, New York, 1987); H. Bohr, G. Rajasekaran, Phys. Rev. **D 32** (1985) 1547, ibid 1553.

[5] J. Kogut, L Susskind, Phys. Rev. **D 11** (1975) 395.

[6] R. Giles, Phys. Rev. **D 24** (1981) 2160.

[7] C. Rovelli, Quantum Gravity, Cambridge University Press, (2004); A. Ashtekar, Phys. Rev. Letts. **57** (1986) 2244.

[8] R. Gambini, Jorge Pullin, Loops, Knots, Gauge Theories and Quantum Gravity (Cambridge University Press, 2000).

[9] Manu Mathur, J. Phys. **A 38** (2005) 10015-10026.

[10] Manu Mathur, Phys. Lett. **B 640** (2006) 292-296.

[11] H. S. Sharatchandra, Nucl. Phys. **B 196** (1982) 62.

[12] Ramesh Anishetty, H. S. Sharatchandra, Phys. Rev. Letts. **65** (1990) 81; B. Gnanapragasam, H. S. Sharatchandra, Phys. Rev. **D 45** (1992) R1010; Ramesh Anishetty, Phys. Rev. **D 44** (1991) 1895.

[13] F. Gliozzi and M.A. Virasoro, Nucl. Phys. **B 164** (1980) 141.

[14] D. Robson, D. M. Weber, Z. Phys. **C 15** (1982) 199.

[15] W. Furmanski, A. Kolawa, Nucl. Phys. **B 291** (1987) 594.

[16] G. Burgio, R. De. Pietri, H. A. Morales-Tecotl, L. F. Urrutia, J. D. Vergara, Nucl. Phys. **B 566** (2000), 547.

[17] J. Schwinger U.S Atomic Energy Commission Report NYO-3071, 1952 or D. Mattis, *The Theory of Magnetism* (Harper and Row, 1982).

[18] Manu Mathur and H. S. Mani, J. Math. Phys. **43** (2002) 5351; Manu Mathur and Diptiman Sen, J. Math. Phys. **42** (2001) 4181, J. M. Radcliffe, J. Phys. **A 4** (1971) 313-323.

[19] Gambini R, Leal L, Trias A, Phys. Rev. **D 39** (1989) 3127; Bartolo C, Gambini R, Leal L, Phys. Rev. **D 39** (1989) 1756.

[20] J. Greensite, Nucl. Phys. **B 166** (1980) 113; C. Hamer, A. Irving, T. Preece, Nucl. Phys. **B 270** (1986) 536; Schütte D, Weihong Z, Hamer C J, Phys. Rev. **D 55** (1997) 2974; S. Guo et. al., Phys. Rev. **D 49** (1994) 507; C. Llewwllyn-Smith, N. atson, Phys. Letts. **B 302** (1993) 463.

[21] Brügmann B, Phys. Rev. **D 43** (1991) 566.

[22] Loll R. Nucl. Phys **B 368** (1992) 121, Nucl. Phys. **B 400** (1993) 126.

[23] Watson N. J., Phys. Letts. **B 323** (1994) 385; Nucl. Phys. Proc. Suppl. (1995) 39BC 224, hep-th/9408174.

[24] S. Chandrasekharan, U.-J. Wiese, Nucl. Phys. **B 492** (1999) 455; R. Brower, S. Chandrasekharan, U.-J. Wiese, Phys. Rev. **D 60** (1999) 094502-1.

[25] D. A. Varshalovich, A. N. Moskalev and V. K. Khersonskii, *Quantum Theory of Angular Momentum* (World Scientific 1988).

[26] A. P. Yutsis, I. B. Levinson and V. V. Vanagas, *Mathematical Apparatus of the Theory of Angular Momentum* (Israel rogram for Scientific Translations, Jerusalem 1962).

[27] T. Banks, R. Myerson, J. Kogut; Nucl. Phys. **B 129** (1977) 493; J. L. Cardy, Nucl. Phys. **B 205** (1982) 1; Manu Mathur, H. S. Sharatchandra, Phys. Rev. Lett. **66** (1991) 3097.

[28] N. D. Hari Dass, Manu Mathur, gr-qc/0611156, Class. Quantum Grav. **24** (2007) 2179.